PŘÍRODOVĚDECKÁ FAKULTA UNIVERZITY KARLOVY
KATEDRA FYZIKÁLNÍ A MAKROMOLEKULÁRNÍ CHEMIE

BAKALÁŘSKÁ PRÁCE

Kristýna PLUHÁČKOVÁ

PRAHA 2007

KARLOVA UNIVERZITA V PRAZE

Přírodovědecká fakulta

Katedra fyzikální a makromolekulární chemie

Bakalářská práce

TEORETICKÉ STUDIUM NEKOVALENTNÍCH INTERAKCÍ V PATROVÝCH A VODÍKOVĚ VÁZANÝCH KOMPLEXECH

Kristýna Pluháčková

Školitel: Prof. Ing. Pavel Hobza, DrSc.

ÚSTAV ORGANICKÉ CHEMIE A BIOCHEMIE AKADEMIE VĚD ČESKÉ REPUBLIKY

Centrum biomolekul a komplexních molekulových systémů

CHARLES UNIVERSITY IN PRAGUE

Faculty of Science

Department of Physical and Macromolecular Chemistry

Bachelor thesis

THEORETICAL STUDY OF NON COVALENT INTERACTIONS IN SANDWICH AND HYDROGEN BONDED COMPLEXES

Kristýna Pluháčková

Advisor: Prof. Ing. Pavel Hobza, DrSc.

INSTITUTE OF ORGANIC CHEMISTRY AND BIOCHEMISTRY

Center for Complex Molecular Systems and Biomolecules

I confirm that I worked out the presented bachelor thesis solely and all the literature used is properly cited.

Prague, 8.3.2007 Kristýna Pluháčková

First, I would like to thank professor Hobza for his guiding me through quantum chemistry and for his kindness and patience. Next I would like to thank Mrs Černá for her technical support as well as all the members of our team for their help, advice and friendship. At last but not at least I would like to thank my family members and my boyfriend for their support, tolerance and love.

Contents

1 Introduction

Experimental studies of noncovalent complexes are complicated and can not describe various properties of the system. One experiment can not mostly provide an information on structure, geometry, stabilization energy and properties of complexes studied.

On the other hand, quantum chemical studies yield full description of studied complex. We can consistently describe not only structure, geometry and stabilization energy but through a knowledge of wave function also all wanted properties.

In this thesis we investigated two sets of molecular complexes possessing different structures, geometry and interesting properties. In the first part we studied the stabilization energy of stacked complexes consisting of benzene and hexasubstituted benzene. Whereas in the second part we aimed at two hydrogen bonded complexes: one of them being a complex of halothane (widely used anesthetics) with acetone.

1.1. Stacked complexes

The potential energy surface of the benzene dimer possesses two energy minima, i.e. T-shaped and parallel-displaced ones (visualised in Figure 1), having very similar stabilisation energies. The stacked (parallel eclipse) structure, originally believed to be the global minimum, does not represent an energy minimum but corresponds to the saddle point. The explanation is simple: the quadrupole-quadrupole interaction is repulsive for the parallel structure while it is attractive for the former structures.[1] The electrostatic energy is responsible for the structure of the dimer whereas the stabilisation of the dimer is caused by London dispersion energy. In the stacked structure, the attractive dispersion energy and electrostatic repulsion are nearly equivalent. In T-shaped and parallel-displaced structures both electrostatic and dispersion energy contributions are attractive but rather small. Consequently, the total stabilisation energy of the dimer is also rather small (the most accurate values are close to 2 kcal/mol).[2] The stacked structure of the dimer is interesting due to its large attractive dispersion energy. Therefore if we change the repulsive

quadrupole-quadrupole interaction for an attractive one, a dramatic increase of the stabilisation energy results. This makes sense only if different subsystems are used.

One of the simplest cases is the benzene...hexafluorobenzene complex. The quadrupole moment of hexafluorobenzene is in absolute value similar to that of benzene but of the opposite sign. This causes attractive electrostatics interaction which makes the parallel structure the most stable one. Already in 1990s theoretical and experimental studies on hetero-dimers appeared.[3,4] It came out that an important part of the overall stabilisation originates in London dispersion energy. Arene-perfluoroarene stacked complexes were studied recently[5] experimentally and theoretically (empirical force field). It was pointed out that stability of the stacked heterodimer originates mainly in the dispersion energy. Crystal studies of isomorphic compounds show a preference for organization in heterodimers versus homodimers. Quantitative analysis shows[5] a cohesive energy of 5-6 kcal/mol per phenyl ring.

The stabilisation energy of non-covalent complexes strongly depends on the theoretical level used, which is especially true for complexes stabilised by dispersion energy. When passing e.g. from MP2/DZ to MP2/TZ level, the stabilisation energy can increase two to five times. Hence we decided to reinvestigate the benzene...hexafluorobenzene complex. In order to maximise the complex stabilisation energy we included also other hexahalogenbenzenes (Cl, Br, I) as well as hexacyanobenzene. The total stabilisation energy of the complexes considered was determined at the CCSD(T) complete basis set (CBS) limit. It is known now that only this level would ensure reliability of stabilisation energies obtained by excluding their dependence at the AO basis set and amount of correlation energy covered.

Stacking interactions, originating in London dispersion energy, contribute significantly to the stability of the DNA double helix. They play a comparable or perhaps even more important role than hydrogen-bonded interactions between complementary nucleic acid bases. It has been recently shown that stacking energies are much larger than previously calculated, and this finding has changed our opinion on the origin of DNA stabilisation. The application of computational procedures is reported to make the evaluation of the accurate stabilisation energies possible for stacked benzene-containing complexes. This can play an important role in supramolecular construction.

Figure 1 The fully optimized MP2/6-31G structures of the stable conformers of benzene, D represents the horizontal displacement in the parallel-displaced dimer

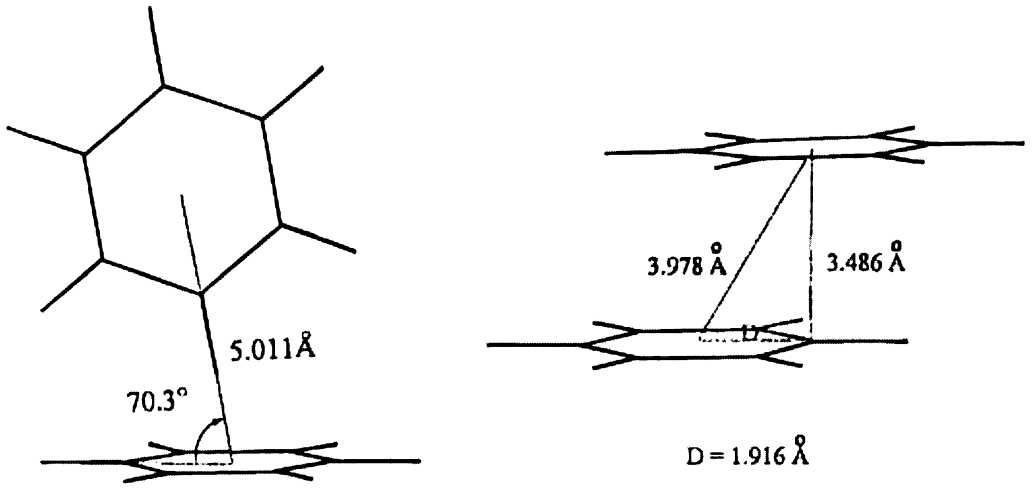

1.2. Hydrogen bonded complexes

The hydrogen(H)- bond is a noncovalent bond between the electron-deficient hydrogen and a region of high electron density. Formation of an H-bond is accompanied by changes in the properties of the X-H covalent bond. Until recently, it was believed that this bond becomes systematically weaker upon complex formation. This is manifested by contraction of the bond and a shift to lower X-H stretching vibration frequencies. A shift to lower frequencies called red shift, represents the most important and easily detectable manifestation of the formation of an H-bond. Red shift was a dogma and none of the three books on H-bonding published at the end of last century[7,8,9] admitted an existence of other than red shift. The first systematic investigation of the opposite, i.e. blue shift of the X-H stretch frequency upon complex formation, was exhibited in a theoretical study of the interaction of benzene with C-H proton donors.[10] Even before this theoretical study a few experimental papers mentioning the existence of blue shift were published. Authors[11] of one of the earliest evidence measured association of fluoroalkanes containing the $-CHF_2$ groups with various proton acceptors and found a shift of the CH stretch frequency to higher values. Fluoroalkanes are used as anaesthetics and their effect is explained by perturbing noncovalent interactions, mainly H-bonding. Among the most potent and

most widely used general anaesthetics belongs halothane (2-bromo-2-chloro-1,1,1-trifluoroethane).

Vibration spectra of halothane and its complexes with acetone and dioxane were measured recently.[12] Contrary to expectations the CH stretch frequency of halothane complexes were shifted to the red (in comparison with the isolated halothane in CCl_4). But the red shifts were rather small (from 6 to 16 cm^{-1}). Experimental CH spectral shifts for several complexes of halogenated proton donors possessing the C-H...O or C-H...π binding motifs are for the sake of comparison presented in Table 1.

Table 1 Experimental spectral shifts of various complexes

	$\Delta\nu_{C\text{-}H}[cm^{-1}]$			
	CH_3COCH_3[a]	CD_3COCD_3[b]	C_2D_4O[b]	Fluorobenzene[c]
HCF_3	17.7	26.7	24.1	21
$HCClF_2$	14.0	24.1	20.7	-
$HCCl_2F$	4.8	15.5	14.2	-
$HCCl_3$	-8.3	0.6	1.3	14

[a] *in liquid argon; Ref. 13;* [b] *in liquid krypton; Ref. 14;* [c] *in gas phase; Ref. 15*

The existence of the red shift in halothane complexes is thus surprising and we decided to investigate its origin in details. Among other reasons such study might put more light on the origin of the blue-shifted H-bonds which, contrary to enormous theoretical and experimental effort, is still not fully understandable. In the present study we investigated the bonding in the halothane...acetone complex and, for the sake of comparison, also in the fluoroform...acetone complex. Let us remind ourselves that fluoroform complexes exhibit a pronounced blue-shifted H-bond.

2 Theoretical methods

2.1. Hartree- Fock approximation

Hartree- Fock approximation is very useful method providing us by a wave function by solving Schrödinger equation. The essence of this approximation is to replace the many-electrons problem by the system of one-electron problems, in which electron moves in an average electric field of other electrons and cores. The simplest antisymmetric wave function for describing the ground state is a single Slater determinant

$$|\psi_0\rangle = |\chi_1\chi_2\cdots\chi_N\rangle \tag{1}$$

The variation principle states that the best wave function of this functional form is the one that gives the lowest possible energy

$$E_0 = \langle\psi_0|\hat{H}|\psi_0\rangle \tag{2}$$

$\hat{H}$ in eq. 2 is the full electronic Hamiltonian. By minimizing E_0 with respect to the choice of spin orbitals one can derive the Hartree-Fock equation that determines the optimal spin orbitals

$$\hat{F}\chi_i = \varepsilon\chi_i \tag{3}$$

where $\hat{F}$ is an effective one- electron operator (Fock operator) of the form

$$\hat{F} = -\frac{\hbar^2}{2m_e}\Delta_i - \sum_i \frac{Ze^2}{4\pi\varepsilon_0 r_i} + \hat{V}_{ee} \tag{4}$$

where Z is a charge of a nucleus, r_i is a distance between the nucleus and an electron i, Δ_i is a Laplac operator and $\hat{V}_{ee}$ is a potential energy of repulsion between an electron and an average electric field made by the others electrons. The Fock operator is the function of the spin orbitals and thus the Hartree-Fock equation is non linear and must be solved iteratively.

However, the Hartree-Fock approximation neglects the instantaneous correlation of the movement of the electrons in the system. The difference between the exact solution and the solution obtained at the Hartree-Fock level is called the correlation energy.

2.2. Møller-Plesset Perturbation theory

The Møller-Plesset method[15] (MP) represents one of the simplest approaches for going beyond the Hartree-Fock approximation to obtain the correlation energy. The principle of this method is to divide the total Hamiltonian into two parts, the zero-order part (H_0) and a perturbation V. H_o is the Hatree-Fock Hamiltonian. The first correction to the Hartree-Fock energy occurs in the second order of perturbation theory and involves a sum over doubly excited determinants. This can be generated by promoting two electrons from occupied orbitals i and j to virtual orbitals a and b. The summation must be restricted so that each excited state is only counted once.

$$E^2 = \sum_{i<j}^{occ} \sum_{a<b}^{vir} \frac{\langle \Phi_0 | \hat{V} | \Phi_{ij}^{ab} \rangle \langle \Phi_{ij}^{ab} | \hat{V} | \Phi_0 \rangle}{E_0 - E_{ij}^{ab}} \tag{5}$$

The correction E^2 is negative and thus in the second order the energy is lowered. MP2 typically accounts for ≈ 80-90% of the correlation energy, and it is the most economical method for including electron correlation.

The MP perturbation method is size extensive but since it is a perturbation method it is possible that the energy will be lower than the exact energy. But this is rarely a problem.

2.2.1 Resolution of Identity Approximation

The resolution of identity approximation (RI) represents a method for making the MP method more efficient and thus less computationally demanding.[16] This method approximate the four center, two electron integrals through the use of the resolution of identity

$$I = \sum_m |m)(m| \tag{6}$$

where $|m)$ represents an orthonormal basis. By inserting the resolution of identity before the two-electron operator one can obtain

$$(ij|kl) = \sum_m (ijm)(m|kl) \tag{7}$$

where (ijm) is a three-center, one electron overlap integral and (m|kl) is a three-center two electron repulsion integral. The benefit of this method comes from the speed of the computation of the integrals. The three-center one-electron overlap integrals are inexpensive to compute and the three-central repulsion integrals are significantly less expensive than the corresponding four-center terms.

2.3. Coupled Clusters Methods

The idea in Coupled Cluster (CC) methods is to include all corrections of a given type to infinite order.[17] The (intermediate normalized) coupled cluster wave function is written as

$$\Psi_{CC} = e^{\hat{T}}\Phi_0$$
$$e^{\hat{T}} = 1 + \hat{T} + \frac{1}{2}\hat{T}^2 + \frac{1}{6}\hat{T}^3 \ldots = \sum_{k=0}^{\infty}\frac{1}{k!}\hat{T}^k \tag{9}$$

where the cluster operator $\hat{T}$ is given by

$$\hat{T} = \hat{T}_1 + \hat{T}_2 + \ldots + \hat{T}_N \tag{10}$$

The T_i operator acting on a HF reference wave function generates all *i*th excited Slater determinants.

With the coupled cluster wave function (8) the Schrödinger equation becomes

$$\hat{H}e^{\hat{T}}\Phi_0 = Ee^{\hat{T}}\Phi_0 \tag{11}$$

and the coupled cluster energy is

$$E_{CC} = \langle\Phi_0|\hat{H}e^{\hat{T}}|\Phi_0\rangle \tag{12}$$

If all cluster operators up to $\hat{T}_N$ are included in $\hat{T}$, all possible excited determinants are generated and the coupled cluster wave function is impossible to be calculated for all but the smallest systems. The cluster operator must be therefore truncated at some excitation level. Since the energy obtained is only approximate. How severe the approximation is depends on how many terms are included in $\hat{T}$. Including only the $\hat{T}_1$ operator does not give any improvement over HF, as matrix elements between the HF and singly excited states are zero. The lowest level of approximation is therefore $\hat{T} = \hat{T}_2$ referred to as Coupled Cluster Doubles (CCD). Using $\hat{T} = \hat{T}_1 + \hat{T}_2$ gives the CCSD model which is only slightly more demanding than CCD, and yields a more complete model. The next higher level has $\hat{T} = \hat{T}_1 + \hat{T}_2 + \hat{T}_3$, giving the CCSDT model.[18] But this involves a computational effort which scales as N^8 (where N is the total number of orbitals). Therefore this method is too computationally expensive. The applicability of CCSD method is limited because it neglects the connected triples. Alternatively the triples contribution can be evaluated by perturbation theory and added to the CCSD results. One of this hybrid methods[19] is CCSD(T). In this method the triples contribution is calculated from the formula given by MP4. In the CCSD(T)

an additional term arising from fifth-order perturbation theory, describing the coupling between singles and triples, is also included.

2.4. Interaction energy

The interaction energy (ΔE) is commonly taken as the energy change upon the formation of the molecular cluster from isolated systems

$$A + B \rightarrow A...B \tag{13}$$

The interaction is thus defined as

$$\Delta E = E(A...B) - [E(A) + E(B)] \tag{14}$$

2.4.1. Basis set superposition error

If the calculations are performed using the variational methods, the interaction energy is influenced by a purely mathematical error that comes from using different basis sets for the subsystems and for the supersystem. This error is referred to as Basis Set Superposition Error (BSSE) and can be eliminated using the Boys and Bernardi function counterpoise method.[20] The interaction energy is evaluated as the difference between the energy of the supersystem and the energies of the subsystems calculated in the basis set of the whole complex.

$$\Delta E^{BSSE} = E(A...B)_{ab} - [E(A)_{ab} + E(B)_{ab}] \tag{15}$$

where an index *ab* denotes the complex geometry.

It is usually observed that the counterpoise correction ($\Delta E^{BSSE} - \Delta E$) for methods including electron correlation is larger and more sensitive to the size of the basis set, than that at the HF level.

Counterpoise correction (CP) can be incorporated to the interaction energy either a posteriori or during the geometry optimalization. Since the second possibility is computationally considerably more demanding if not necessary we use the former method.

2.4.2. CCSD(T) complete basis set (CBS) interaction energy

The CBS CCSD(T) interaction energy is approximated as

$$\Delta E^{CCSD(T)}{}_{CBS} = \Delta E^{MP2}{}_{CBS} + (\Delta E^{CCSD(T)} - \Delta E^{MP2})|_{\text{medium basis set}} \tag{16}$$

where the first and second term represent the complete basis set (CBS) limit of the MP2 interaction energy and the CCSD(T) correction term.

The CCSD(T) correction term is calculated with the medium basis set (6-31G*). This can be done, because the [CCSD(T)-MP2] interaction energy difference depends much less on the basis set than the MP2 and CCSD(T) interaction energies themselves.[21] More details on the construction of CCSD(T) CBS interaction energies can be found in the Jurečka and Hobza paper.[22]

2.4.3. Extrapolation of stabilization energy to a complete basis set

The MP2 stabilisation energy is extrapolated to the CBS limit using the two-point scheme of Helgaker and co-workers.[23,24] Because of different convergence of the Hartree-Fock (HF) and MP2 energies, both energies are always extrapolated to their CBS limits separately.

$$E_{CBS}^{HF} = E_{X}^{HF} - Ae^{-\alpha X} \quad \text{and} \quad E_{CBS}^{Corr} = E_{X}^{corr} - AX^{-3} \tag{16}$$

where E_X and E_{CBS} are HF and correlation energies for the basis set with the principal quantum number X, and at the complete basis set limit, respectively. A and α are adjustable parametres.

In a paper[22] on DNA base pairs the authors compared MP2/CBS interaction energies obtained from two points extrapolations based on aug-cc-pVDZ and aug-cc-pVTZ energies as well as on aug-cc-pVTZ and aug-cc-pVQZ energies. The latter extrapolation being considerably more expensive yields very similar results as the previous one and the difference between both values never exceeds 3% of the total stabilization energy.

2.4.4. Deformation energy

The deformation energy of monomers A and B upon formation a molecular complex (A...B) is defined as

$$E_{def} = \left|E(A) - E(A)_{ab}\right| + \left|E(B) - E(B)_{ab}\right| \tag{17}$$

where an index *ab* denotes the complex geometry. The energies of each monomer must be computed in the same basis so that we do not have to deal with some additional BSSE. The deformation energy is always positive and thus contributes to the repulsion of subsystems.

2.5. Natural Bond Orbital Analysis

The concept of natural orbitals may be used for distributing electrons into atomic and molecular orbitals, and thereby for deriving atomic charges and molecular bonds. The idea in the *Natural Atomic Orbital* (NAO) and *Natural Bond Orbital* (NBO) analysis developed by F. Weinholt and co-workers[25] is to use one-electron density matrix for defining the shape of the atomic orbitals in the molecular environment, and derive molecular bonds from electron density between atoms.

The density matrix can be written in terms of blocks of basis functions belonging to a specific centre as

$$\hat{D} = \begin{pmatrix} \hat{D}^{AA} & \hat{D}^{AB} & \hat{D}^{AC} & \ldots \\ \hat{D}^{BA} & \hat{D}^{BB} & \hat{D}^{BC} & \ldots \\ \hat{D}^{CA} & \hat{D}^{CB} & \hat{D}^{CC} & \ldots \\ \ldots & \ldots & \ldots & \ldots \end{pmatrix} \tag{8}$$

The Natural Atomic Orbitals for atom A in the molecular environment may be defined as those which diagonalize the $\hat{D}^{AA}$ block but these orbitals need to be orthogonalized so that the orbital occupation numbers would sum to the total number of electrons. At first each of the atomic blocks in the density matrix is diagonalized to produce a set of non-orthogonal NAOs, often denoted as "pre-NAOs". Next the strongly occupied (i.e. having occupation numbers significantly different from zero) and weakly occupied (i.e. having occupation numbers close to zero) pre-NAOs are made orthogonal separately. The final set of orthogonal orbitals are simply denoted NAOs, and the diagonal elements of the density matrix in this basis are orbital population.

Once the density matrix has been transformed to the NAO basis, bonds between atoms may be identified from the off-diagonal blocks. The procedure involves the following steps.

a) NAOs for an atomic block in the density matrix which have occupation numbers very close to 2 (say > 1.999) are identified as core orbitals. Their contributions to the density matrix are removed.

b) NAOs for an atomic block in the density matrix which have large occupancy numbers (say > 1.90) are identified as lone pair orbitals. Their contributions to the density matrix are also removed.

c) Each pair of atoms (AB, AB, BC, ...) is now considered, and the two-by-two subblocks of the density matrix (with the core and lone pair contributions removed) are diagonalized. Natural bond orbitals are identified as eigenvectors which have large eigenvalues (occupation numbers larger than say 1.9).

d) If an insufficient number of NBOs are generated by the above procedure (sum of occupation numbers for core, lone pair and bond orbitals significantly less than the number of electrons), the criteria for accepting a NBO may be gradually lowered until a sufficient large fraction of the electrons has been assigned to bonds. Alternatively a search may be initiated for three-center bonds. The contributions to the density matrix from all diatomic bonds are removed, and all three-by-three subblocks are diagonalized. Such three-centre bonds are quite rare, boron systems being the most notable exception.

Once NBOs have been identified, they may be written as linear combinations of the NAOs, forming a localized picture if the "atomic" orbitals are involved in the bonding.

Population analyses based on basis functions (such as Mulliken or Lőwdin) require insignificant computational time although they are shortcomings. Therefore the NAO procedure is an attractive method for analysis purposes. But for modeling purposes (i.e. force field charges) ESP charges are clearly the logical choice.

2.6. Density functional theory

The basis for Density Functional Theory (DFT) is the proof by Hohenberg and Kohn[26] that the ground-state electronic energy is determined completely by the electron density ρ. In other words, there exists a one-to-one correspondence between the electron density of a system and the energy. The significance of this is perhaps best illustrated by comparing to the wave function approach. A wave function for an N-electron system contains $3N$ coordinates, three for each electron (four if spin is included). The electron density is the square of the wave function, integrated over N-1 electron coordinates, this only depends on three coordinates, independently of the number of electrons. The "only" problem is that although it has been proven that each different density yields a different ground-state energy, the functional connecting these two quantities is not known. The goal of DFT methods is to design functionals connecting the electron density with the energy.[27]

In Generalized Gradient Approximation (GGA) method the exchange and correlation energies depend not only on the electron density but also on derivatives of the density. GGA methods are also sometimes referred to as non-local methods although this is somewhat misleading since the functionals depend only on the density (and derivatives) at a given point, not on a space volume as for example the Hartree-Fock exchange energy.

One of the GGA functionals is the PW91 introduced by Perdew and Wang in 1991.[28] In general it is found that the GGA methods often give geometries and vibrational frequencies for stable molecules of the same or better quality than MP2, at a computational cost similar to HF. For systems containing multi-reference character, where MP2 usually fails badly, DFT methods are often found to generate results of a quality comparable to that obtained with coupled cluster methods.[29]

The inclusion of the correlation energy, faster basis set convergence compared to other methods and the relatively cheap computational demands make DFT methods increasingly popular amongst the chemical community. However, until recently[30] the most serious drawback of the DFT methods was either widely ignored or it was stated that the DFT can not be used for specific chemical and biophysical problems. This drawback is the fact that the dispersion interactions, which have non-local character, cannot be described by local functional of the electron density. Different methods to account for dispersion term or improving the functional form were developed. Unfortunately, only few of them were particularly successful when applied to a wide range of organic molecules.

On of the successful method is standard density functional theory augmented with a damped empirical dispersion term made by Jurečka, Černý et al.[31] The aim of their work was to suggest a computationally efficient empirical model with good transferability and reasonable small error. They have added to the total DFT energy dispersion energy

$$E_{dis} = -\sum_{ij} f_{damp}(r_{ij}, R_{ij}^0) C_{6ij} r_{ij}^{-6} \tag{9}$$

where $r_{ij,}$ is the interatomic distance and R_{ij}^0 is the equilibrium van der Waals (wdW) separation derived from the atomic vdW radii. A particular dispersion scheme is defined by a set of the atomic dispersion coefficients C_{6ij}, a set of the vdW radii R_{ij}^0,

and by dumping function f_{damp}. Authors used a set of C_{6ij} coefficients and a dumping function tested by Grimme.[32]

2.7. Symmetry adapted perturbation theory

In symmetry adapted perturbation theory[33] (SAPT) the total interaction energy, E_{int}, is obtained as a sum of separately calculated first-order electrostatic, $E_{el}^{(1)}$, and second order induction and dispersion contributions, $E_{ind}^{(2)}$ and $E_{disp}^{(2)}$, respectively. All of these terms do contain the corresponding penetration contributions and the (second-order) charge-transfer contribution is included in $E_{ind}^{(2)}$. Furthermore these terms are accompanied by corresponding first-, $E_{exch}^{(1)}$, and second-order exchange-corrections, $E_{exch-ind}^{(2)}$ and $E_{exch-disp}^{(2)}$, respectively, describing the repulsive effects of electron exchange between the overlapping molecular charge distribution. In particular for hydrogen-bridges induction, exchange-induction and charge-transfer effects of higher than second-order in the intermolecular perturbation operator become non-negligible, their combined effect can be estimated from supermolecular Hartree-Fock calculations and then is denoted as $\delta(HF)$.

$$E_{\text{int}}^{(2)} = E_{el}^{(1)} + E_{exch}^{(1)} + E_{ind}^{(2)} + E_{exch-ind}^{(2)} + E_{disp}^{(2)} + E_{exch-disp}^{(2)} + \delta(HF) \qquad (18)$$

In the conventional SAPT based on the double-perturbation theory,[33] the intra- and intermolecular perturbation is treated separately, what is declared by using two numbers in the exponent of the interaction energy components, first for the intra-, and second for the intermolecular perturbation order. This exact and accurate approach is unfortunately prohibitively demanding. However, thanks to the combination of a DFT treatment of monomer properties with a SAPT treatment of intermolecular interaction (DFT-SAPT)[34] and the introduction of the density-fitting approximation, the SAPT calculations with extended basis sets on medium-sized systems such as the benzene dimer recently have become possible.[35] A similar method was developed also by group of the authors of the original SAPT treatment.[36] Because the perturbation theory exploits virtual orbitals the inherently incorrect DFT orbitals need to be corrected in some way. Hasselmann and Janssen used a gradient-controlled shift procedure[37] which needs a difference (shift) between the experimental vertical ionization potential and HOMO energy of the DFT method used as an input.

3 Calculations

3.1. Stacked complexes

3.1.1 The investigated complexes

We investigated stacked structures of complexes formed by benzene with hexasubstituted benzenes. For the sake of comparison the stacked structure of the benzene dimer was studied as well. Stacked structures of the $C_6H_6...C_6X_6$ (X= F, Cl, Br, I, CN) complexes are visualised in Figure 2.

3.1.2. Structures

Structures of all subsystems were determined by gradient optimization using MP2 method with SDD** basis set and RI-MP2 method with cc-pVTZ basis set. Structures of all complexes were determined at the same levels; standard gradient optimization was used for the former procedure while the counterpoise-corrected gradient optimization for the latter one. For all systems considered the C_{6v} symmetry was maintained.

3.1.3. Properties of subsystems

The subsystem properties are used only for qualitative discussion and thus only rather low-level calculations had been performed. Specifically, quadrupole moments of all subsystems (with exception of hexaiodobenzene) were evaluated at the Hartree-Fock level with cc-pVTZ basis set. Polarisabilities of isolated subsystems were calculated at the MP2 level with cc-pVDZ basis set.

3.1.4. Interaction energy

The MP2 stabilisation energy is extrapolated to the CBS limit using the two-point scheme of Helgaker and co-workers.[23,24] Because of different convergency of the Hartree-Fock (HF) and MP2 energies, both energies were extrapolated to their CBS limits separately on the basis of the aug-cc-pVDZ and aug-cc-pVTZ energies.[38]

The CCSD(T) correction term is calculated with the medium basis set and basis sets like 6-31G*, 6-31G** and cc-pVDZ provide similar results. In our study we used the 6-31G* basis set. The use of medium basis set is justified because the

[CCSD(T)-MP2] interaction energy difference depends much less on the basis set than the MP2 and CCSD(T) interaction energies themselves.[21]

All interaction energies were corrected for the basis set superposition error and the frozen core approximation was systematically applied. When the standard gradient optimization was used (MP2/SDD** calculations) the systematically repulsive deformation energies were taken into consideration. MP2/cc-pVTZ deformation energies were added to all CBS interaction energies.

3.1.5. Decomposition of total interaction energy

The total interaction energies were decomposed to their components using the DFT-SAPT perturbation treatment.[33,34,35,39] The DFT-SAPT calculations were carried out for the benzene dimer and also for the complexes of benzene with hexafluorobenzene, hexachlorobenzene and hexacyanobenzene, taking the CP-corrected RI-MP2/cc-pVTZ geometries, which were previously shown to be more accurate than the RI-MP2/cc-pVTZ geometries[34]. We used PBE0AC exchange-correlation functional with density fitting and aug-cc-pVDZ basis set for the decomposition. The aug-cc-pVDZ set is large enough to give reliable estimate of the electrostatic, induction and exchange components (the SAPT calculations are not burdened with the basis set superposition error). The dispersion component is underestimated by about 10-20 % in this basis[39] but it should serve well for the purpose of comparison of the relative dispersion magnitudes.

Because perturbation theory exploits orbital energies the inherently incorrect DFT orbitals (both occupied and virtual) need to be corrected in some way. Hesselmann and Janssen used a gradient-controlled shift procedure[36,34] which needs a difference (shift) between the vertical ionization potential (IP) and HOMO energy of the DFT method used as an input. Herein the IPs were calculated at the PBE0/TZVP level, while the HOMO values were taken from the aug-cc-pVDZ calculation. Our shift values were 0.0715, 0.0690, 0.0539, and 0.0515 E_h for benzene, hexafluorobenzene, hexachlorobenzene, and hexacyanobenzene, respectively. Unfortunately we were unable to perform the decomposition for the brominated benzene due to software problems.

3.1.6. Relativistic calculations

Relativistic effects play an important role in heavier halogens. The structures of studied complexes were optimized at the MP2 level using the Stuttgart-Dresden basis set which uses for elements heavier than Ar pseudopotentials (SDD)[40] ; the core basis sets (D95V for H,C,N,F,Cl and [2s3p] for Br and I) were augmented by two sets of polarisation functions at halogens, carbons, nitrogens and hydrogens [(C, N, F, Cl, Br, I, H) = 0.8, 0.25; 0.8, 0.25; 0.8, 0.25; 0.6, 0.15; 0.5, 0.1; 0.4, 0.07; 1.0, 0.15]. Stabilisation energies of these complexes were determined at the same level and the BSSE corrections and deformation energies were systematically included.

The TURBOMOLE,[41] MOLPRO[42] and GAUSSIAN03[40] codes were used in this part of work.

Figure 2 Optimized structures of all investigated stacked complexes

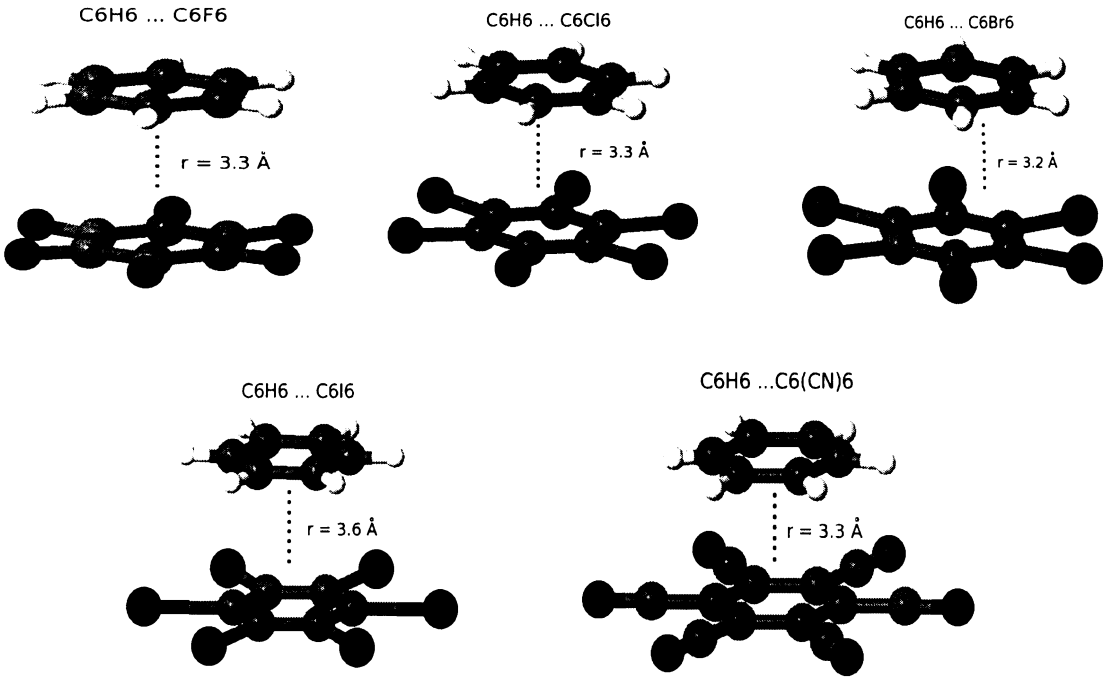

3.2. Hydrogen bonded complexes

3.2.1. Properties of subsystems as well as complexes

Subsystem (halothane, fluoroform, acetone) as well as complex (halothane...acetone, fluoroform...acetone) geometries were optimized at the RI-MP2/cc-pVTZ level. The standard gradient optimization technique was adopted.

Stabilization energies of both complexes were determined at the same level and the basis set superposition error (BSSE) was included a posteriori.

Harmonic vibration frequencies were obtained at the same theoretical level and no scaling was adopted.

3.2.2. NBO analysis

To learn more about the nature of complexation the Natural Bond Orbital (NBO) analysis was performed. The method is fully defined only when based on Hartree-Fock and DFT characteristics. The subsystems and all complexes were therefore reoptimized at the DFT/TPSS/TZVP level and all NBO results were determined at the DFT/B3-LYP/cc-pVTZ level.

3.2.3. SAPT analysis

The total interaction energies were decomposed to their components using the DFT-SAPT perturbation treatment.[33,34,35,39] We used PBE0AC exchange-correlation functional with density fitting and the aug-cc-pVDZ basis set for the decomposition. The aug-cc-pVDZ set is large enough to provide a reliable estimate of the electrostatic, induction and exchange components. The dispersion component is underestimated by about 10–20% in this basis set but should serve well enough for the purpose of comparison. We implemented a gradient-controlled shift procedure which needs a difference (shift) between the vertical ionisation potential (IP) and HOMO energy of the DFT method used as an input.[43] The IPs were calculated at the PBE0/TZVP level while the HOMO values were taken from the aug-cc-pVDZ calculation.

All calculations were performed with TURBOMOLE[42] and GAUSSIAN03[40].

4 Results and discussion

4.1. Stacked complexes[a]

4.1.1. Properties of subsystems

Table 2 shows quadrupole moments and polarisabilities of the subsystems studied.

The quadrupole moments of hexacyanobenzene and hexafluorobenzene are the largest ones and because of their opposite sign to benzene quadrupole the electrostatics interactions are large and attractive. Considering only the simple electrostatics the sandwich complexes of benzene with hexacyanobenzene and hexaflurobenzene are the most stable.

The polarisabilities of benzene and hexafluorobenzene are similar while that of hexachlorobenzene, hexabromobenzene and hexacyanobenzene are much higher. With growing polarisabilities of subsystems the London dispersion interaction is getting stronger (see eq. 19) and stabilises the dimer.

$$E^D = -\frac{3}{2} \cdot \frac{\alpha_A \alpha_B}{R^6} \cdot \frac{c_A c_B}{c_A + c_B} \tag{19}$$

where R is the distance between subsystems, α_A (α_B) polarisability and $c_A(c_B)$ are mostly approximated by the ionization potentials of isolated subsystems.

Table 2 Quadrupole moments (Q, a.u.) and polarisabilities (α,Å^3) of C_6X_6 (X=H, F, Cl, Br, CN) systems

	Q [a.u.]	α [Å^3]
C_6H_6	-6.59	56.23
C_6F_6	7.89	57.24
C_6Cl_6	0.25	120.63
C_6Br_6	-4.72	152.93
C_6CN_6	28.23	148.81

[a] For more information see the Appendix A.

4.1.2. Interaction energies

Table 3 shows interaction energies of stacked structures determined at various levels.

The aug-cc-pVDZ and aug-cc-pVTZ values of the HF interaction energies differ only slightly and, consequently, the CBS limit is also rather similar. The HF interaction energies are systematically repulsive. It is at first sight surprising because attractive electrostatic quadrupole-quadrupole energy was expected. It must be, however, kept in mind that the HF interaction energy includes besides the electrostatic term also induction and exchange-repulsion terms. The attractive electrostatic term is compensated by the repulsive exchange-repulsion term.

The MP2 correlation interaction energies (cf. Table 3) depend more on the quality of the basis set than the HF interaction energy and the non-negligible difference between the CBS limit and the aug-cc-pVTZ value illustrates the importance of CBS extrapolation. The MP2 correlation stabilisation energy is large and increases from the benzene through the hexafluoro- and hexachloro- to the hexabromobenzene. This behaviour basically corresponds to polarisabilities of the substituted benzenes.

When passing from the fluoro- to the cyano-isomer the MP2 stabilisation energy significantly increases, namely from 8.5 to 15.7 kcal/mol, i.e. by almost 90 %.

Table 3 shows that the CCSD(T) correction term is repulsive and for the hexabromobenzene complex it is by far the largest among all the existing values (DNA base pairs, amino acid pairs). The final stabilisation energies are thus smaller than the MP2/CBS ones but they are still substantial. The largest value (more than 11 kcal/mol) was determined for the hexacyanobenzene complex, followed by the hexachlorobenzene and hexabromobenzene complexes. Large repulsive CCSD(T) correction term for the hexabromobenzene complex explains the fact that total stabilization energy of this complex is smaller than that of the hexachlorobenzene complex.

Passing from the fluorobenzene to the bromobenzene the MP2 stabilisation energy of stacked dimers increases significantly, and the question arises what happens when the iodobenzene is considered. However, the relativistic effects play an important role there and so the non-relativistic calculations cannot be used. Table 3 summarises the MP2/SDD** results (effectively covering the relativistic effects for bromobenzene and iodobenzene) for all complexes. A direct comparison between the CBS and

MP2/SDD** values is difficult. We can only compare the changes when passing from one halogen to the other one. In both calculations the bromobenzene...benzene stabilization energies are smaller than that of chlorobenzene...benzene. This trend follows even for hexaiodobenzene complex (SDD** calculations). Investigating the MP2/SDD** stabilisation energies, we found that they increase from F to Cl but decrease for I. We can thus conclude that relativistic effects are responsible for lower stabilization of hexaiodobenzene complex.

Table 3 Hartree-Fock (HF), MP2 correlation (COR) and total (Tot) interaction energies, and CCSD(T) interaction energies evaluated with various basis sets[a] for the stacked structures of the $C_6 H_6$... $C_6 X_6$ (X=H, F, Cl, Br, I, CN) complexes; the numbers in parentheses refer to the CCSD(T) correction term (energies in kcal/mol)

		MP2[b]			SDD** [c]	CCSD(T)
X		**aD[a]**	**aT[a]**	**CBS[d]**		
H	HF	*5.91*	*5.79*	*5.76*	-1.08	-
	COR	*-8.8*	*-9.04*	*-9.21*		
	Tot	**-2.89**	**-3.25**	**-3.45**		
F	HF	*4.87*	*5.01*	*5.05*	-4.88	**-6.32** (2.18)
	COR	*-12.11*	*-12.99*	*-13.63*		
	Tot	**-7.24**	**-7.98**	**-8.50**		
Cl	HF	*7.92*	*8.05*	*8.08*	-7.93	**-8.75** (4.00)
	COR	*-18.74*	*-19.99*	*-20.91*		
	Tot	**-10.82**	**-11.94**	**-12.75**		
Br	HF	*8.61*	*8.73*	*8.76*	-7.80	**-8.10** (5.73)
	COR	*-20.18*	*-21.60*	*-22.64*		
	Tot	**-11.57**	**-12.87**	**-13.83**		
CN	HF	*3.48*	*3.52*	*5.54*	-	**-11.01** (4.65)
	COR	*-17.38*	*-18.60*	*-19.49*		
	Tot	**-13.90**	**-15.08**	**-15.66**		
I	-				-7.78	-

[a] *aD and aT denote aug-cc-pVDZ and aug-cc-pVTZ basis sets, whereas CBS refers to a complete basis set, and SDD indicates Stuttgart and Dresden pseudopotentials*

[b] *MP2/cc-pVTZ interaction energies and deformation energies for complexes mentioned amount to -3.44, 0.002; -7.29, 0.08; -10.75, 0.07; -11.91, 0.05; and -14.21, 0.30 kcal/mol, respectively.*

[c] *Deformation energies for all complexes (with exception of hexacyanobenzene one) equal to 0.01, 0.39, 0.37, 0.36, and 0.11 kcal/mol, respectively, and are included.*

[d] *CBS interaction energies corrected for the MP2/cc-pVTZ deformation energies*

4.1.3. SAPT analysis

From the previous part it is obvious that decomposition of the total interaction energy into physically correct energy terms is important for explanation of the nature of stabilisation of the complexes under study.

From the Table 4 it is evident that the electrostatic $E^{(1)}_{pol}$ term is systematically stabilizing for all clusters studied. The first order interaction energies (the sums of polarization and exchange-repulsion terms, $E^{(1)}$ in Table 4) are, however, systematically repulsive. This is caused by large repulsion values of the exchange-repulsion terms.

Second-order induction term is surprisingly large but summing this term with its exchange counterpart we obtain negligible contribution. On the other hand the second-order dispersion term is always large and significant. Dispersion energy for the hexachlorobenzene and the hexacyanobenzene complexes is similar which is slightly surprising in the light of much larger polarisability of the hexacyanobenzene. Exchange-dispersion term is systematically small. The second-order interaction energies ($E^{(2)}$ in Table 4) are for all complexes attractive and their major part originates in dispersion energy.

Putting all energy terms (including the δHF one) together we obtain the total interaction energy which can be compared only with the sum of ΔE^{MP2} (aug-cc-pVDZ) and $\Delta E^{CCSD(T)}$ energies. The SAPT stabilisation energy is slightly smaller (by 0.4 kcal/mol) for the $C_6H_6...C_6F_6$ complex and larger (by 1.2 and 2.6 kcal/mol) for $C_6H_6...C_6Cl_6$ and $C_6H_6...C_6(CN)_6$ complexes, respectively. The differences are not dramatic and agreement between both stabilization energies is satisfactory.

Table 4 The SAPT decomposition of interaction energy of the stacked structures of the $C_6H_6...C_6X_6$ (X= H, F, Cl, Br, CN) complexes (energies in kcal/mol)

	$E^{(1)}_{pol}$	$E^{(1)}_{exch}$	$E^{(1)}$	$E^{(2)}_{ind}$	$E^{(2)}_{ind-exch}$	$E^{(2)}_{dis}$	$E^{(2)}_{disp-exch}$	$E^{(2)}$	δHF	E_{INT}
H	-0.74	5.96	**5.32**	-2.09	1.94	-7.12	1.06	**-6.21**	-0.16	**-1.14**
F	-6.36	12.12	**5.76**	-6.83	6.47	-11.32	1.72	**-9.95**	-0.51	**-4.70**
Cl	-5.41	10.59	**5.19**	-4.70	4.26	-13.99	1.77	**-12.67**	-0.50	**-7.98**
CN	-8.97	11.1	**2.14**	-5.95	4.30	-13.45	1.63	**-13.47**	-0.55	**-11.88**

4.2. Hydrogen bonded complexes[b]

4.2.1. Properties of subsystems

Figure 3 and Table 5 show structure, geometry, dipole moments and selected stretching vibration frequencies of isolated subsystems. The dipole moment of fluoroform, which is larger than that of halothane, indicates weaker electrostatic interactions in the halothane...acetone complex than in fluoroform...acetone complex.

Very important property that frequently determines the character of the H-bonding is the change of the molecule dipole moment in consequence of the change of X-H bond length. Most often, this change is positive what means that elongation of the X-H bond is connected with the dipole moment increase. Several systems exhibit, however, an opposite feature and the dipole moment increase is connected with contraction of the X-H bond.

However, with halothane the situation is different. Both elongation as well as contraction of the C-H bond (by 0.1 Å) gives dipole moment increase (1.39 D and 1.35 D).

Table 5 Structure, dipole moments and selected stretching vibration frequencies of isolated subsystems

	μ[D]	$\nu_{C\text{-}H}$[cm^{-1}]	$r_{C\text{-}H}$[Å]
Halothane	1.24	3183	1.084
Fluoroform	1.67	3204	1.085
Acetone	2.97		

[b] For more information see the Appendix B.

Figure 3 Structures and geometries of isolated subsystems

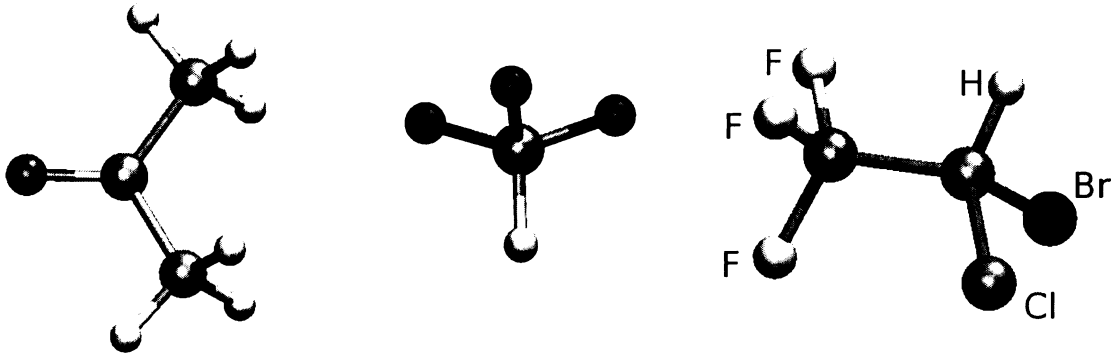

Acetone Fluoroform Halothane

4.2.2. Properties of complexes and interaction energies

Figure 4 and Table 6 show structure, geometry and selected stretch vibration frequencies of the fluoroform...acetone and halothane...acetone complexes determined at the MP2 and DFT levels. The MP2 entries will be discussed first. The C-H...O hydrogen bond in the halothane....acetone complex is nearly linear and the distance between heavy atoms (3.09 Å) indicates an existence of rather strong bonding. This is confirmed by substantial stabilization energy of the complex which amounts to 5 kcal/mol. The C-H bond in halothane is slightly contracted upon complexation (by 0.002 Å) and the bond contraction indicates a blue shift of the C-H stretch frequency. To our surprise the resulting C-H stretch vibration frequency is red shifted and the shift is not negligible (27 cm^{-1}). The C=O bond in acetone is also contracted upon complexation (by 0.005 Å) and its stretch frequency is only slightly red-shifted (by 3 cm^{-1}).

From the Figure 4 it is evident that the complex of fluoroform with acetone exhibits practically linear C-H...O hydrogen bond and also the distance of heavy atoms is comparable (3.26 Å) to the halothane...acetone complex. The C-H bond is contracted upon complexation and the contraction is the same as in the case of previous complex. Performing the vibration analysis we found a pronounced blue shift of 36 cm^{-1}. The stabilization energy of the latter complex is slightly smaller (3.66 kcal/mol) but the difference is not substantial. When investigating the composition of the stabilization energies we have found an important difference. The correlation part of the stabilization energy of the halothane complex amounts to 3.3 kcal/mol while in the case of fluoroform complex it is only 0.2 kcal/mol. Further, the Hartree-Fock (HF)

stabilization energy of the halothane complex (1.66 kcal/mol) is considerably smaller than that of fluoroform complex (3.45 kcal/mol). These numbers indicate that the binding in the halothane complex originates in correlation energy while in the case of the fluoroform complex it comes from the HF energy.

Table 6 Structure and selected stretch vibration frequencies of the fluoroform...acetone and halothane...acetone complexes determined at the MP2 and DFT levels

		$r_{C\text{-}H}$[Å]	$\nu_{C\text{-}H}$[cm^{-1}]	ΔE(kcal/mol)[a]
Halothane...acetone	MP2	1.082	3156	-5.0/-1.7/-3.3
	DFT	1.091	3053	-4.2
Fluoroform...acetone	MP2	1.083	3240	-3.7/-3.5/-0.2
	DFT	1.091	3121	-4.0

[a]*Total interaction energy/HF interaction energy/correlation interaction energy*

Figure 4 Structure and geometry of the fluoroform...acetone and halothane...acetone complexes

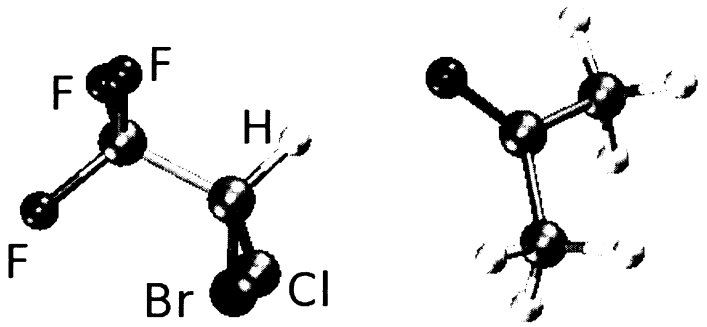

Halothane...acetone

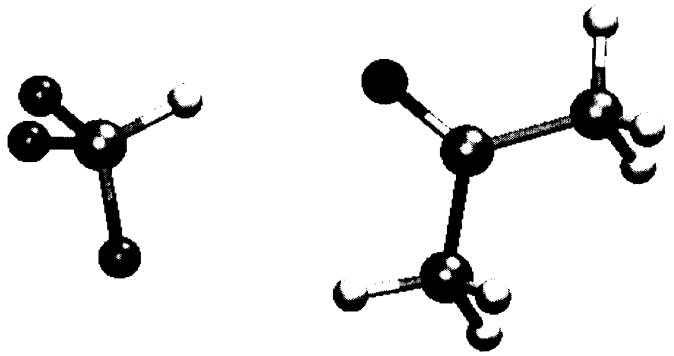

Fluoroform...acetone

4.2.3. NBO analysis

Table 7 shows that MP2 and DFT characteristics and spectral shifts are similar for both complexes. The DFT blue shift in the fluoroform...acetone complex is slightly smaller than the MP2 one while the DFT red shift in the halothane...acetone complex is larger than the MP2 one. This fact is important since it indicates that it is possible to use the DFT technique in the subsequent NBO analysis.

Table 7 shows the changes of electron density in both complexes investigated. Both complexes exhibit the same trend of charge transfer (CT), a flow from acetone to proton donor. Halothane attracts 0.013 e while the CT in the case of fluoroform is about one half (0.007 e). Different magnitudes of the CT are reflected by different stabilization energies of both complexes. Though these characteristics are not exactly proportional this ratio indicates important role of charge-transfer-based energy contributions. Investigating the second-order charge-transfer energies in both complexes we found dominant contribution from acetone oxygen lone pair → C-H σ* antibonding orbital of the proton donor. This term is about twice larger for the halothane complex (5.1 and 2.6 kcal/mol) and indicates that the more favourable geometrical arrangement of the halothane...acetone complex is responsible for higher stabilization energy of the halothane complex.

Investigating the electron density (ED) at the acetone oxygen we found almost twice larger decrease in halothane complex. The ED in the C-H σ* antibonding orbital of the fluoroform decreases upon complexation with acetone which indicates the strengthening and contraction of the bond connected with the blue shift of the C-H stretch frequency. Investigating the ED in other σ* antibonding orbitals in fluoroform we found even larger decrease in two of three C-F orbitals. Decrease of ED in C-H and two C-F σ* antibonding orbitals is compensated by an ED increase in lone electron pairs of all three fluorines. The overall picture is thus the same we know from other fluoroform...proton acceptor complexes. The NBO analysis clearly indicates a decrease of ED in the C-H σ* antibonding orbital of fluoroform leading to bond contraction and a blue shift of the respective stretching frequency.

In the halothane complex we found an opposite effect, the ED in the C-H σ* antibonding orbital of the halothane increased what indicates weakening and elongation of the bond connected with the red shift. Calculations as well as experiment indicate the red shift but they differ in the absolute values. The change of

ED in the C-H σ* antibonding orbital of halothane is about six times larger than that in fluoroform. Consequently, larger spectral shifts can be expected in the halothane complex. From the Table 6 we learned, however, that this is not true and the absolute shift is larger in the fluoroform complex. These numbers tells us clearly that the mechanism of the H-bonding in both complexes has to be different.

To explain this difference we investigated the changes in hybridization upon complex formation. The carbon in isolated halothane possesses $sp^{2.60}$ hybridization. Upon complexation the hybridization decreases to $sp^{2.35}$. Lowering of the hybridization is connected with the strengthening of the bond and its contraction. Performing the same analysis for the fluoroform we found similar though slightly smaller trend: the carbon hybridization decreases upon complexation from $sp^{2.30}$ to $sp^{2.15}$. Putting both effects together we found their collateral action in the case of fluoroform complex while in the case of halothane complex they act contradictorily. Evidently, the halothane...acetone complex is characterised by compensation of substantial hyperconjugation mechanism leading to red shift of the C-H stretch frequency and of substantial rehybridization mechanism leading to blue shift of the C-H stretch frequency. The resulting calculated shift is small and red which agrees with experimental finding. In the case of fluoroform complex both mechanisms are going hand-in-hand and the resulting shift is blue and it is relatively large.

Table 7 MP2 and DFT characteristics of both fluoroform...acetone and halothane...acetone complexes

Halothane...acetone			
Halothane		Acetone	
orbital	ΔED [e⁻]	orbital	ΔED [e⁻]
LP (Cl)	0.00232	$BD(C^3\text{-}H^9)$	-0.00949
$BD^*(C\text{-}H)$	0.00600	$BD(C^4\text{-}H^6)$	-0.00700
$BD^*(C\text{-}C)$	-0.00227	$LP(O^2)$	-0.00441
		$BD^*(C^1\text{-}O^2)$	0.01110
		$BD^*(C^1\text{-}C^3)$	-0.00457
		$BD^*(C^1\text{-}C^4)$	-0.00437

Fluoroform...acetone			
Fluoroform		Acetone	
Fluoroform	ΔED [e⁻]	orbital	ΔED [e⁻]
LP(F)	0.00728	$BD^*(C^1\text{-}C^3)$	-0.00358
		$BD^*(C^1\text{-}O^2)$	0.00781
		$BD^*(C^1\text{-}C^4)$	-0.00332

ΔED is defined as a difference between electron density of the orbital in dimer and monomer. Acetone is labelled in the figure 5

Figure 5 Labelling of atoms in the acetone molecule

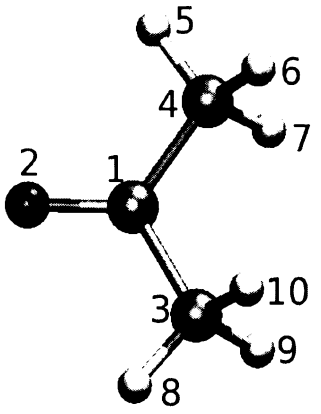

4.2.4. SAPT analysis

To understand the difference in the nature of the stabilisation of the halothane...acetone and fluoroform...acetone complexes we have performed the DFT-SAPT calculations. The energies obtained are shown in Table 8. Although total interaction energies differ slightly from the supermolecular values given in Table 6 they serve very well for the sake of comparison between complexes. The difference mentioned can be explained by different basis sets used in the supermolecular (cc-pVTZ) and perturbation (aug-cc-pVDZ) calculations.

Investigating the entries in Table 8 we found comparably attractive electrostatic energies but considerably different exchange-repulsion energies for both complexes. Consequently, the $E^{(1)}$ energies are attractive for the fluoroform...acetone complex but repulsive for the halothane...acetone complex. The difference is considerable; more than 4 kcal/mol in favour of the fluoroform complex. For both complexes, the second-order induction energies are rather small and significant stabilisation

originates in the second-order dispersion energies. The dispersion energy of the halothane complex is more than twice that of the fluoroform complex.

The DFT-SAPT energy components fully support the decomposition of the variation interaction energy mentioned in the previous paragraph. However, we were not able to deduce the nature of the spectral shift of the proton donor upon complexation on the basis of energy decomposition. Evidently, the subtle differences in the C-H stretch frequencies cannot be explained on the basis of total interaction energies or their components.

Table 8 The DFT-SAPT analysis for the halothane...acetone and fluoroform...acetone complexes; energies in kcal/mol

	$E^{(1)}_{pol}$	$E^{(1)}_{exch}$	$E^{(1)}$	$E^{(2)}_{ind+ind\text{-}exch}$	$E^{(2)}_{disp+disp\text{-}exch}$	$E^{(2)}$	δHF	E_{INT}
Fluoroform ...acetone	-6.08	5.36	**-0.72**	-0.77	-2.42	**-3.19**	-0.51	**-4.41**
Halothane ...acetone	-5.88	9.77	**3.89**	-1.55	-5.38	**-6.92**	-1.31	**-4.35**

5 Conclusions

5.1. Stacked complexes

1. The CCSD(T)/CBS stabilisation energies of $C_6H_6...C_6X_6$ (X= F, Cl, Br, I, CN) complexes are very large (between 6.3 and 11.0 kcal/mol), much larger than previously determined.

2. The largest stabilisation energy found for the benzene…hexacyanobenzene complex is a result of attractive dispersion and electrostatic quadrupole-quadrupole energies; the former term is the dominant attractive contribution. Large attraction in the stacked arrangement requires a concerted (attractive) action of electrostatic and London dispersion contributions. Rather large attraction originating from polarization and induction contributions is compensated by their exchange counterparts.

3. The stabilisation energy of the benzene…hexaiodobenzene is lower than that of the Br isomer, which is explained by relativistic effects.

4. The stabilisation energies of the stacked complexes are substantial, which suggests that this motif and these constructing blocks may be considered as a powerful tool in supramolecular construction requiring the stable orientation of molecular subsystems. The $C_6 H_6... C_6 X_6$ (X= F, Cl, Br, I, CN) recognition motif shows a significant stabilization well comparable with hydrogen bonding. The stacking interactions thus exhibit comparable supramolecular activity as hydrogen bonding which was believed to be the only recognition factor.

5.2. Hydrogen bonded complexes

1. Halothane is (to our knowledge) the first system exhibiting positive as well as negative dipole moment derivatives. When we both shorten or lengthen the C-H bond the halothane dipole moment increases. As a consequence of this behaviour one cannot expect pronounced spectral shift (either red or blue) of the halothane upon complexation.

2. Calculated spectral shift of the halothane...acetone complex agrees well with the experimental data.

3. Surprisingly small red shift of the C-H stretch frequency of halothane resulting from complexation with acetone was explained by compensation by hyperconjugation and rehybridization mechanisms.

4. Fluoroform...acetone complex exhibited blue shift of the C-H stretch frequency upon complexation and in this case hyperconjugation as well as rehybridization mechanisms act in coincidental action.

5. The origin of blue-shifting H-bonding in various types of complexes formed by polar as well as nonpolar subsystems is explained by the hyperconjugation/rehybridization model of Alabugin et al.[44,45] and the repulsion-wall model introduced in Ref. 10.

List of abbreviations

6-31G*	Pople´s basis set containing one set of polarization functions
AO	Atomic orbitals
aug-cc-pVDZ	Dunning´s basis set[38] of Double Zeta quality containing diffuse functions
aug-cc-pVTZ	Dunning´s basis set[38] of Triple Zeta quality containing diffuse functions
B3-LYP	hybrid functionals, which include a mixture of Hartree-Fock exchange with DFT exchange-correlation[46]
BSSE	Basis Set Superposition Error
CBS	Complete Basis Set limit
CCSD(T)	Coupled Clusters theory calculating Single and Double excitations and taking triple excitations from MP4
CT	Charge transfer
DFT	Density Functional Theory
DNA	Deoxyribonucleic acid
ED	Electron density
GGA	Generalized Gradient Approximation methods
H-bond	Hygrogen bond
HF	Hartree-Fock theory
HOMO	Highest Occupied Molecular Orbital
IP	Ionization Potential
MP2	Møller-Plesset method concerning second correction term
NAO	Natural Atomic Orbital
NBO	Natural Bond Orbital analysis
PBE	The 1996 functional of Perdew, Burke and Ernzerhof[47,48]
RI	Resolution of Identity approximation
SAPT	Symmetry Adapted Perturbation Theory
SDD	Stutgard-Dresden basis set
TPSS	The τ-dependent gradient-corrected functional of Tao, Perdew, Staroverov, and Scuseria[49]
TZVP	*Ahlrichs's valence basis of triple zeta quality*

References

1. Müller-Dethlefs, K.; Hobza, P. *Chem. Rev.* **2000**, 100, 143.
2. Sinnokrot, M.O.; Sherill, C.D. *J. Am. Chem. Soc.* **2004**, 126, 7690.
3. Williams, J.H. *Acc. Chem. Res.* **1993**, 26, 593.
4. West, Jr. A.P.; Mecozzi, S.; Dougherty, D.A. *J. Phys. Org. Chem.* **1997**, 10, 347.
5. Bacchi, S.; Benaglia, M.; Cozzi, F.; Demartin, F.; Filippini, G.; Gavezzotti, A. *Chem. Eur. J.* **2006**, 12, 3538.
6. (a) Šponer, J.; Hobza, P. *Coll. Czech. Chem. Commun.* 2003, 68, 2231; (b) Hobza, P.; Šponer, J. *Chem. Rev.* **1999**, 99, 3247.
7. Jeffrey, G.A. An introduction to hydrogen bonding, *Oxford University Press,* New York, **1997**.
8. Desiraju, G.R.; Steiner, T. The weak hydrogen bond. *Oxford University Press,* Oxford, **1999**.
9. Scheiner, S. Hydrogen bonding. *Oxford University Press,* New York, **1997**.
10. Hobza, P.; Špirko, V.; Selzle, H. L.; Schlag, E. W. *J. Phys. Chem. A* **1998**, 102, 2501.
11. Trudeau, G. T.; Dumas, J.-M.; Dupuis, P.; Guerin, M.; Sandorfy, C. *Top. Curr. Chem.* **1980**, 93, 91.
12. Czarnik-Matusewicz, B.; Michalska, D.; Sandorfy, C.; Zeegers-Huyskens, Th. *Chem. Phys.* **2006**, 322, 331.
13. Delanoye, S. N.; Herrebout, W. A.; van der Veken, B. J. *J. Am. Chem. Soc.* **2002**, *124,* 7490.
14. Hobza, P.; Havlas Z. Chem. Rev. **2000**, 100, 4253
15. Møller, C. and Plesset, M. S., *Phys. Rev.,* **1934**, 46, 618.
16. Feyereisen.
17. Bartlett, R. J. *J.Phys.Chem.,* **1989**, 93, 1697.
18. Watts, J. D. and Barlett, R. J. *Int. J. Quantum Chem.,* **1993**, S27, 51.
19. Scuseria, G. E. and Lee, T. J., *J. Phys. Chem.,* **1990**, 93, 5851.
20. Boys, S. F. and Bernardi, F. *Molecular Physics* **1970**, 19, 553.
21. Jurečka, P.; Hobza, P., Chem. Phys. Letters 2002, 365, 89.
22. Jurečka, P.; Hobza, P., *J. Am. Chem. Soc.* **2003,** *125*, 15608.

23. Halkier, A.; Helgaker, T.; Jorgensen, P.; Klopper, W.; Koch, H.; Olsen, J.; Chem. Phys. Lett. **1998**, 286, 243-252.
24. Halkier, A.; Helgaker, T.; Jorgensen, P.; Klopper, W.; Olsen, J.;, Chem. Phys. Lett. **1999**, 302, 437
25. Reed, A. E.; Curtiss, L. A. and Weinholt, F. *Chem. Rev.,* **1988**, 88, 899.
26. Hohenberg, P. and Kohn, W. *Phys. Rev.* **1964**, 136, B864.
27. Parr, R. G. and Yang, W. *Density Functional Theory,* Oxford University Press, 1989.
28. Perdew, J.P.; Chavary, J.A.; Vosko, S. H.; Jackson, K. A.; Pederson, M. R.; Singh, D. J. and Fiolhais, J. P., *Phys. Rev. B,* **1992**, 46, 6671.
29. Oliphant, N. and Bartlett, R. J., *J. Chem. Phys.,* **1994**, 100, 6550.
30. Hobza, P.; Šponer, J.; Rechel, T.; *J. Comput. Chem.,* **1995**, 16, 1315.
31. Jurečka, P.; Černý, J.; Hobza, P.; Salahub, D. R., *J. Comput. Chem*, 28, **2007**, 555-569.
32. Grimme, S. J., *J. Comput. Chem.,* **2004**, 25, 1463.
33. Jeziorski, B.; Moszynski, R.; Szalewicz, K. *Chem. Rev.* **1994**, 94, 1887.
34. (a)Jansen, G.; Hesselmann, A. *J. Phys. Chem. A* **2001**, 105, 11156. (b) Hesselmann, A.; Jansen, G. *Chem. Phys. Lett.* **2002,** 357, 464. (c) Hesselmann, A.; Jansen, G. *Chem. Phys. Lett.* **2002**, 362, 319. (d) Hesselmann, A.; Jansen, G. *Chem. Phys. Lett.* **2003**, 367, 778. (e) Hesselmann, A.; Jansen, G. *Phys. Chem. Chem. Phys.* **2003**, 5, 5010.
35. Hesselmann, A.; Jansen, G.; Schűtz M. *J. Chem. Phys.* **2005,** 122, 014103.
36. Podeszva, R.; Bukowski, R.; Szalewicz, K. *J. Chem. Theory Comput.*, **2006**, 2, 400.
37. Grünig, M.; Gritsenko, O. V.; van Ginsbergen, S. J. A.; Baerends, E. J. *J. Chem. Phys.* **2001**, 114, 652.
38. Dunning, T.H. *J. Chem. Phys.* **1989,** 90, 1007.
39. Dąbkowska, I.; Jurečka, P.; Hobza, P., *J. Chem. Phys.* **2005**, 122, 204322.
40. Gaussian 03, Revision C.02, Frisch, M. J.; Trucks, G. W.; Schlegel, H. B.; Scuseria, G. E.; Robb, M. A.; Cheeseman, J. R.; Montgomery, Jr., J. A.; Vreven, T.; Kudin, K. N.; Burant, J. C.; Millam, J. M.; Iyengar, S. S.; Tomasi, J.; Barone, V.; Mennucci, B.; Cossi, M.; Scalmani, G.; Rega, N.; Petersson, G. A.; Nakatsuji, H.; Hada, M.; Ehara, M.; Toyota, K.; Fukuda, R.; Hasegawa, J.; Ishida, M.; Nakajima, T.; Honda, Y.; Kitao, O.; Nakai, H.; Klene, M.; Li, X.;

Knox, J. E.; Hratchian, H. P.; Cross, J. B.; Bakken, V.; Adamo, C.; Jaramillo, J.; Gomperts, R.; Stratmann, R. E.; Yazyev, O.; Austin, A. J.; Cammi, R.; Pomelli, C.; Ochterski, J. W.; Ayala, P. Y.; Morokuma, K.; Voth, G. A.; Salvador, P.; Dannenberg, J. J.; Zakrzewski, V. G.; Dapprich, S.; Daniels, A. D.; Strain, M. C.; Farkas, O.; Malick, D. K.; Rabuck, A. D.; Raghavachari, K.; Foresman, J. B.; Ortiz, J. V.; Cui, Q.; Baboul, A. G.; Clifford, S.; Cioslowski, J.; Stefanov, B. B.; Liu, G.; Liashenko, A.; Piskorz, P.; Komaromi, I.; Martin, R. L.; Fox, D. J.; Keith, T.; Al-Laham, M. A.; Peng, C. Y.; Nanayakkara, A.; Challacombe, M.; Gill, P. M. W.; Johnson, B.; Chen, W.; Wong, M. W.; Gonzalez, C.; and Pople, J. A.; Gaussian, Inc., Wallingford CT, **2004**.

41. Ahlrichs, R.; Bär, M.; Häser, M.; Horn, H.; Kölmel, C.; *Chem. Phys. Lett.* **1989**, 162, 165.
42. MOLPRO, version 2006.1, a package of *ab initio* programs, Werner, H.-J.; Knowles, P. J.; Lindh, R.; Manby, F. R.; Schütz, M.; Celani, P.; Korona, T.; Rauhut, G.; Amos, R. D.; Bernhardsson, A.; Berning, A.; Cooper, D. L.; Deegan, M. J. O.; Dobbyn, A. J.; Eckert, F.; Hampel, C. and Hetzer, G.; Lloyd, A. W.; McNicholas, S. J.; Meyer, W. and Mura, M. E.; Nicklass, A.; Palmieri, P.; Pitzer, R.; Schumann, U.; Stoll, H.; Stone, A. J.; Tarroni, R. and Thorsteinsson, T. **2006**
43. Hesselmann, A.; Jansen, G.; *Phys. Chem. Chem. Phys.* **2003**, 5, 5010, and references therein.
44. Alabugin, I. V.; Manoharan, M.; Peabody, S.; Weinhold, F. *J. Am. Chem. Soc.* **2003**, 125, 5973.
45. Alabugin, I. V.; Manoharan, M.;Weinhold, F. *J. Phys. Chem. A* **2004**, 108, 4270.
46. Becke, A. D. *J. Chem. Phys.* **1998**, 5648 (1993).
47. Perdew, J. P.; Burke, K.; and Ernzerhof, M. *Phys. Rev. Lett.* **1977**, 3865 (1996).
48. Perdew, J. P.; Burke, K.; and Ernzerhof, M. *Phys. Rev. Lett* . **1978**, 1396 (1997).
49. Tao, J. M.; Perdew, J. P.; Staroverov, V. N. and Scuseria, G. E. *Phys. Rev. Lett.*, **1991**, 146401 (2003).
50. Schaefer, A.; Horn, H. and Ahlrichs, R. *J. Chem. Phys.* **97**, 2571 (1992).

Appendices – Attached Publications

Appendix A

K. Pluháčková, P. Jurečka and P. Hobza, "Stabilization energy of $C_6H_6...C_6X_6$ (X = F, Cl, Br, I, CN) complexes: complete basis set limit calculations at MP2 and CCSD(T) levels", *Physical Chemistry Chemical Physics* ***9****, pp. 755-760 (2007)*

Stabilisation energy of $C_6H_6\cdots C_6X_6$ (X = F, Cl, Br, I, CN) complexes: complete basis set limit calculations at MP2 and CCSD(T) levels†

Kristýna Pluháčková,[a] Petr Jurečka[b] and Pavel Hobza*[ab]

Received 20th October 2006, Accepted 30th November 2006
First published as an Advance Article on the web 19th December 2006
DOI: 10.1039/b615318f

Stabilisation energies of stacked structures of $C_6H_6\cdots C_6X_6$ (X = F, Cl, Br, CN) complexes were determined at the CCSD(T) complete basis set (CBS) limit level. These energies were constructed from MP2/CBS stabilisation energies and a CCSD(T) correction term determined with a medium basis set (6-31G**). The former energies were extrapolated using the two-point formula of Helgaker *et al.* from aug-cc-pVDZ and aug-cc-pVTZ Hartree–Fock energies and MP2 correlation energies. The CCSD(T) correction term is systematically repulsive. The final CCSD(T)/CBS stabilisation energies are large, considerably larger than previously calculated and increase in the series as follows: hexafluorobenzene (6.3 kcal mol^{-1}), hexachlorobenzene (8.8 kcal mol^{-1}), hexabromobenzene (8.1 kcal mol^{-1}) and hexacyanobenzene (11.0 kcal mol^{-1}). MP2/SDD** relativistic calculations performed for all complexes mentioned and also for benzene···hexaiodobenzene have clearly shown that due to relativistic effects the stabilisation energy of the hexaiodobenzene complex is lower than that of hexabromobenzene complex. The decomposition of the total interaction energy to physically defined energy components was made by using the symmetry adapted perturbation treatment (SAPT). The main stabilisation contribution for all complexes investigated is due to London dispersion energy, with the induction term being smaller. Electrostatic and induction terms which are attractive are compensated by their exchange counterparts. The stacked motif in the complexes studied is very stable and might thus be valuable as a supramolecular synthon.

Introduction

The potential energy surface of the benzene dimer possesses two energy minima, *i.e.* T-shaped and parallel-displaced ones, having very similar stabilisation energies. The stacked (parallel eclipse) structure, originally believed to be the global minimum, does not represent an energy minimum but corresponds to the saddle point. The explanation is simple, the quadrupole–quadrupole interaction (quadrupole being the first non-zero multipole moment) is repulsive for the parallel structure while it is attractive for the former structures.[1] It is the electrostatic energy that is responsible for the structure of the dimer, whereas the stabilisation of the dimer is due to London dispersion energy (the electrostatic contribution is smaller). In the stacked structure, the dispersion energy is largest among all structures (maximal overlap of both subsystems), but electrostatic repulsion is also large here. Electrostatic and dispersion energy contributions in T-shaped and parallel-displaced structures are attractive but are, due to the large distance between the centres of mass of both subsystems, rather small. Consequently, the total stabilisation energy of the dimer is also rather small (the most accurate values are close to 2 kcal mol^{-1}).[2] The parallel structure of the dimer is interesting due to its large dispersion energy; providing that we can change the repulsive quadrupole–quadrupole interaction for an attractive interaction, a dramatic increase of the stabilisation energy should result. This is certainly impractical for the dimers made by identical subsystems but in the case of different subsystems it is viable.

The simplest case is the benzene···hexafluorobenzene complex. The quadrupole moment of hexafluorobenzene is in absolute value similar to that of benzene but of the opposite sign. This means that the stacked structure of the hetero-dimer possesses an attractive quadrupole–quadrupole electrostatic term, whereas in the case of the T-shaped and parallel-displaced ones this term is repulsive. This is nothing new and Williams[3] already in the 1990s pointed out a higher melting point of the co-crystal of the two compared with either pure compound. The first theoretical studies on hetero-dimer appeared also in the 1990s,[4] with the authors reporting "fairly strong stabilisation" of about 3.7 kcal mol^{-1} (MP2/6-31G** level). It was concluded that an important part of the overall stabilisation originates in London dispersion energy. Arene–perfluoroarene stacked complexes were studied recently[5] experimentally and theoretically (empirical force field) and it was pointed out that stability of the stacked heterodimer originates mainly in the dispersion energy. Crystal studies of

[a] *Institute of Organic Chemistry and Biochemistry, Academy of Sciences of the Czech Republic and Centre for Biomolecules and Complex Molecular Systems, Flemingovo nám. 2, 166 10 Prague 6, Czech Republic. E-mail: pavel.hobza@uochb.cas.cz*
[b] *Department of Physical Chemistry, Palacky University, tr. Svobody 26, 771 46 Olomouc, Czech Republic*
† Electronic supplementary information (ESI) available: Counterpoise-corrected geometries. See DOI: 10.1039/b615318f

isomorphic compounds show a preference for organization in heterodimers *versus* homodimers. Quantitative analysis shows[5] a cohesive energy of 20–25 kJ mol^{-1} per phenyl ring.

The stabilisation energy of non-covalent complexes strongly depends on the theoretical level used, which is especially true for complexes stabilised by dispersion energy. When passing, *e.g.*, from MP2/DZ to MP2/TZ level, the stabilisation energy can increase two to five times. In the light of this fact, we decided to reinvestigate the benzene···hexafluorobenzene complex. Additionally, in order to maximise the complex stabilisation energy, we also included, besides the hexafluorobenzene, other hexahalogenbenzenes (Cl, Br, I) as well as hexacyanobenzene. The total stabilisation energy of the complexes considered was determined at the CCSD(T) complete basis set (CBS) limit.

Stacking interactions, originating in London dispersion energy, contribute significantly to the stability of the DNA double helix and play a comparable or even more important role than hydrogen-bonded interactions between complementary nucleic acid bases. We have recently shown that stacking energies are large,[6] much larger than previously calculated, and this finding has changed our opinion on the origin of DNA stabilisation. In this paper we report the application of computational procedures making it possible to evaluate accurate stabilisation energies for stacked benzene-containing complexes which can play a role in supramolecular construction.

Calculations

The complexes investigated

We investigated stacked structures of complexes formed by benzene with hexasubstituted benzenes. For the sake of comparison the stacked structure of the benzene dimer was studied as well. Stacked structures of the $C_6H_6\cdots C_6X_6$ (X = F, Cl, Br, I, CN) complexes are visualised in Fig. 1.

Structures

Structures of all subsystems were determined by gradient optimization using MP2 method with SDD** basis set and

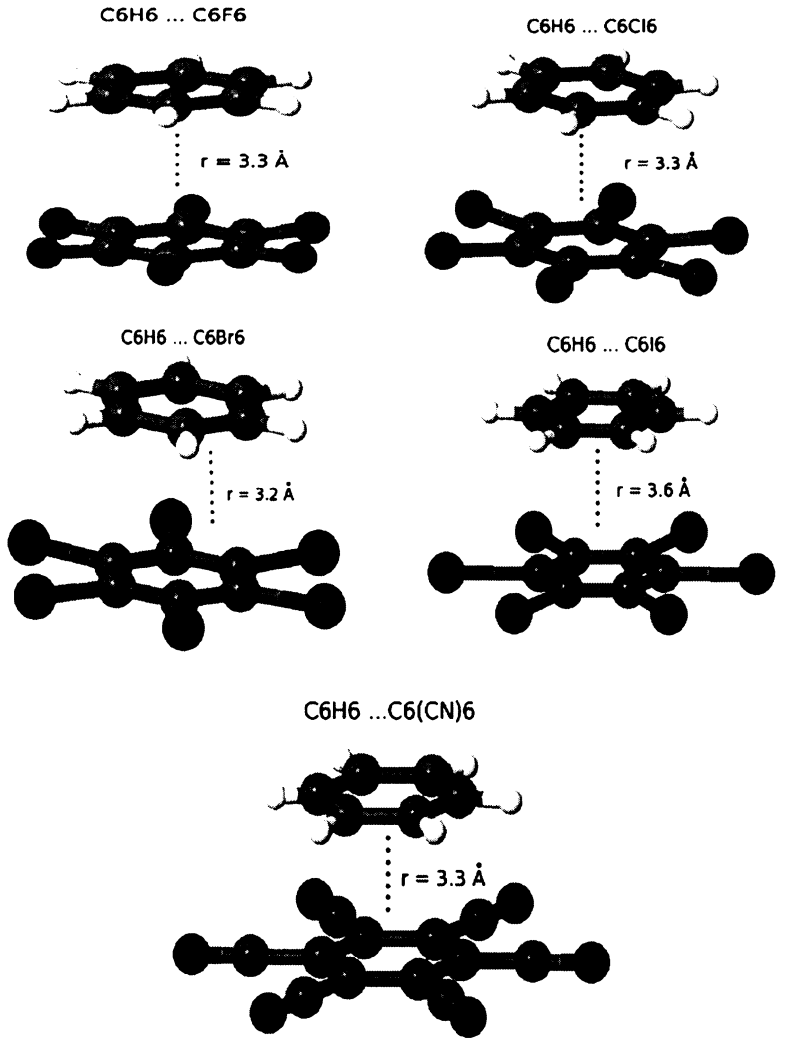

Fig. 1 Optimized structures of all complexes investigated.

RI-MP2 method with cc-pVTZ basis set. Structures of all complexes were determined at the same levels; standard gradient optimization was used for the former procedure while the counterpoise-corrected gradient optimization for the latter one. For all systems considered the C_{6v} symmetry was maintained.

Subsystem properties

The subsystem properties will be used only for qualitative discussion and thus only rather low-level calculations were performed. Specifically, the quadrupole moments of all subsystems (with the exception of hexaiodobenzene) were evaluated at the Hartree–Fock level with cc-pVTZ basis set. Polarisabilities of isolated subsystems were calculated at the MP2 level with cc-pVDZ basis set.

CCSD(T) CBS interaction energies

The CBS CCSD(T) interaction energy is approximated as

$$\Delta E_{\mathrm{CBS}}^{\mathrm{CCSD(T)}} = \Delta E_{\mathrm{CBS}}^{\mathrm{MP2}} + (\Delta E^{\mathrm{CCSD(T)}} - \Delta E^{\mathrm{MP2}})|_{\mathrm{medium\ basis\ set}}, \quad (1)$$

where the first and second terms represent the CBS limit of the MP2 interaction energy and the CCSD(T) correction term. These energies were systematically evaluated for (standard) RI-MP2/cc-pVTZ structures.

The MP2 stabilisation energy is extrapolated to the CBS limit using the two-point scheme of Helgaker and co-workers.[7,8] Because of different convergency of the Hartree–Fock (HF) and MP2 energies, both energies were extrapolated to their CBS limits separately on the basis of the aug-cc-pVDZ and aug-cc-pVTZ energies.[9] In our previous paper on DNA base pairs[10] we compared MP2/CBS interaction energies obtained from two points extrapolations based on aug-cc-pVDZ and aug-cc-pVTZ energies as well as on aug-cc-pVTZ and aug-cc-pVQZ energies. The latter extrapolation, being considerably more expensive, yields very similar results as the previous one: the difference between both values never exceeds 3% of the total stabilization energy.

The CCSD(T) correction term is calculated with the medium basis set and basis sets like 6-31G*, 6-31G** and cc-pVDZ provide similar results. In our study we used the 6-31G* basis set since this basis set was used in our previous paper.[11] The use of medium basis set is justified because the [CCSD(T)-MP2] interaction energy difference depends much less on the basis set than the MP2 and CCSD(T) interaction energies themselves.[11] More details on the construction of CCSD(T) CBS interaction energies can be found in our previous work.[10]

All interaction energies were corrected for the basis set superposition error, and the frozen core approximation was systematically applied. When the standard gradient optimization was used (MP2/SDD** calculations) the systematically repulsive deformation energy (difference between the energy of isolated optimized subsystem and subsystem in the complex geometry) was taken into consideration. MP2/cc-pVTZ deformation energies were added to all CBS interaction energies.

Decomposition of total interaction energy

The total interaction energies were decomposed to their components using the DFT-SAPT perturbation treatment.[12–16] The DFT-SAPT calculations were carried out for the benzene dimer and also for the complexes of benzene with hexafluorobenzene, hexachlorobenzene and hexacyanobenzene, taking the CP-corrected RI-MP2/cc-pVTZ geometries, which were previously shown to be more accurate than the RI-MP2/cc-pVTZ geometries.[17] (Counterpoise-corrected geometries are given in the ESI.†) We used PBE0AC exchange–correlation functional with density fitting and aug-cc-pVDZ basis set for the decomposition. The aug-cc-pVDZ set is large enough to give reliable estimate of the electrostatic, induction and exchange components (note that the SAPT calculations are not burdened with the basis set superposition error). The dispersion component is underestimated by about 10–20% in this basis[12] but it should serve well for the purpose of comparison of the relative dispersion magnitudes.

In SAPT the total interaction energy E_{int} is calculated as a sum of the electrostatic, exchange, induction and dispersion components, the dispersion and induction components having also their exchange counterparts:

$$E_{\mathrm{int}} = E_{\mathrm{pol}}^{1} + E_{\mathrm{ex}}^{1} + E_{\mathrm{ind}}^{2} + E_{\mathrm{ex\text{-}ind}}^{2} + E_{\mathrm{disp}}^{2} + E_{\mathrm{ex\text{-}disp}}^{2} + \Delta\mathrm{HF}. \quad (2)$$

In the conventional SAPT based on the double-perturbation theory,[13] the intra- and intermolecular perturbations are treated separately, what is declared by using two numbers in the exponent of the interaction energy components, first for the intra-, and second for the intermolecular perturbation order. This exact and accurate approach is unfortunately prohibitively demanding. Here we employed a DFT flavour of the SAPT method by Hesselmann and Janssen[12,14–16] in which the intramolecular correlation is treated fully by DFT, while the intermolecular interaction is left to intermolecular perturbation theory. The exponents in eqn (2) thus refer to the intermolecular perturbation order only. A similar method was developed also by group of the authors of the original SAPT treatment.[18] Because perturbation theory exploits orbital energies the inherently incorrect DFT orbitals (both occupied and virtual) need to be corrected in some way. Hesselmann and Janssen used a gradient-controlled shift procedure[19] which needs a difference (shift) between the vertical ionization potential (IP) and HOMO energy of the DFT method used as an input. Herein the IPs were calculated at the PBE0/TZVP level, while the HOMO values were taken from the aug-cc-pVDZ calculation. Our shift values were 0.0715, 0.0690, 0.0539, and 0.0515 E_{h} for benzene, hexafluorobenzene, hexachlorobenzene, and hexacyanobenzene, respectively. Unfortunately, we were unable to perform the decomposition for the brominated benzene due to software problems. For details on the use of density fitting, auxiliary basis, and local exchange see the original paper.[12]

Relativistic calculations

Relativistic effects play an important role with heavier halogens. The structures of complexes studied were optimized at

the MP2 level using the Stuttgart–Dresden basis set which uses for elements heavier than Ar pseudopotentials (SDD);[20] the core basis sets (D95V for H,C,N,F,Cl and [2s3p] for Br and I) were augmented by two sets of polarisation functions at halogens, carbons, nitrogens and hydrogens [(C, N, F, Cl, Br, I, H) = 0.8, 0.25; 0.8, 0.25; 0.8, 0.25; 0.6, 0.15; 0.5, 0.1; 0.4, 0.07; 1.0, 0.15]. The stabilisation energies of these complexes were determined at the same level and the BSSE corrections and deformation energies were systematically included.

The TURBOMOLE,[21] MOLPRO[22] and GAUSSIAN03[20] codes were used throughout the paper.

Results and discussion

Subsystems

Table 1 shows quadrupole moments and polarisabilities of the subsystems studied. Evidently, the quadrupole moments of benzene and hexafluorobenzene are similar but with the opposite sign while that of hexachlorobenzene practically vanishes. The quadrupole moment of hexabromobenzene is again negative but smaller than that of hexafluorobenzene. As expected, the quadrupole moment of hexacyanobenzene is by far the largest and is positive. On the basis of a simple electrostatic consideration, sandwich complexes of benzene with hexacyanobenzene and hexaflurobenzene will be the most stable.

The polarisabilities of benzene and hexafluorobenzene are similar while those of hexachlorobenzene, hexabromobenzene and hexacyanobenzene are much higher.

Table 1 Quadrupole moments (Q, au) and polarisabilities (α, Å^3) of C_6X_6 (X = H, F, Cl, Br, CN) systems

System	Q	α
C_6H_6	−6.59	56.23
C_6F_6	7.89	57.24
C_6Cl_6	0.25	120.63
C_6Br_6	−4.72	152.93
$C_6(CN)_6$	28.23	148.81

Complexes

Table 2 shows interaction energies of stacked structures determined at various levels, including the CBS one. Let us recall that all-electron calculations were performed for geometries determined by counterpoise-corrected RI-MP2/cc-pVTZ optimizations while the pseudopotentials used geometries from standard gradient optimizations performed at MP2/SDD** level. The HF interaction energies will be discussed first. The aug-cc-pVDZ and aug-cc-pVTZ values differ only slightly and, consequently, the CBS limit is also rather similar. This indicates that already the aug-cc-pVDZ basis set yields HF interaction energies close to saturation. The HF interaction energies are systematically repulsive, and the largest repulsion was found for the hexabromobenzene complex, followed by the hexachlorobenzene one. The repulsion of hexafluorobenzene and hexacyanobenzene complexes is comparable. The fact that the HF interaction energy for all present complexes is repulsive (at the MP2 geometries) is at first sight

Table 2 Hartree–Fock (HF), MP2 correlation (COR) and total (Tot) interaction energies, and CCSD(T) interaction energies evaluated with various basis sets[a] for the stacked structures of the $C_6H_6\cdots C_6X_6$ (X = H, F, Cl, Br, I, CN) complexes; the numbers in parentheses refer to the CCSD(T) correction term (energies in kcal mol^{-1})

	MP2[b]					
X		aD	aT	CBS[d]	SDD** [c]	CCSD(T)
H	HF	*5.91*	*5.79*	*5.76*	−1.08	—
	COR	*−8.80*	*−9.04*	*−9.21*		
	Tot	**−2.89**	**−3.25**	**−3.45**		
F	HF	4.87	5.01	5.05	−4.88	**−6.32** (2.18)
	COR	*−12.11*	*−12.99*	*−13.63*		
	Tot	**−7.24**	**−7.98**	**−8.50**		
Cl	HF	7.92	8.05	8.08	−7.93	**−8.75** (4.00)
	COR	*−18.74*	*−19.99*	*−20.91*		
	Tot	**−10.82**	**−11.94**	**−12.75**		
Br	HF	8.61	8.73	8.76	−7.80	**−8.10** (5.73)
	COR	*−20.18*	*−21.60*	*−22.64*		
	Tot	**−11.57**	**−12.87**	**−13.83**		
CN	HF	3.48	3.52	5.54	—	**−11.01** (4.65)
	COR	*−17.38*	*−18.60*	*−19.49*		
	Tot	**−13.90**	**−15.08**	**−15.66**		
I	—				−7.78	—

[a] aD and aT denote aug-cc-pVDZ and aug-cc-pVTZ basis sets, whereas CBS refers to a complete basis set, and SDD indicates Stuttgart and Dresden pseudopotentials. [b] MP2/cc-pVTZ interaction energies and deformation energies for complexes mentioned amount to −3.44, 0.002; −7.29, 0.08; −10.75, 0.07; −11.91, 0.05; and −14.21, 0.30 kcal mol^{-1}, respectively. [c] Deformation energies for all complexes (with exception of hexacyanobenzene one) equal to 0.01, 0.39, 0.37, 0.36, and 0.11 kcal mol^{-1}, respectively, and are included. [d] CBS interaction energies corrected for the MP2/cc-pVTZ deformation energies.

surprising, because attractive electrostatic quadrupole–quadrupole energy was expected. It must be, however, kept in mind that the HF interaction energy includes besides the electrostatic term also induction and exchange-repulsion terms, and the attractive electrostatic term is compensated by the repulsive exchange-repulsion term. The decomposition of the total interaction energy will be discussed later.

The MP2 correlation interaction energies (*cf.* Table 2) depend more on the quality of the basis set than on the HF interaction energy but even in this case the dependence is not dramatic. Passing from the aug-cc-pVDZ to the much larger aug-cc-pVTZ basis set results in about a 10% increase in the MP2 correlation stabilisation energy. The CBS limit is still larger, and the non-negligible difference between it and the aug-cc-pVTZ value illustrates the importance of CBS extrapolation. The MP2 correlation stabilisation energy is large and increases from the benzene through the hexafluorobenzene and hexachlorobenzene to the hexabromobenzene, which basically corresponds to polarisabilities of the substituted benzenes. The MP2 correlation stabilisation energy evidently includes not only the London dispersion energy but also intrasystem correlation energy contributions.

The MP2 CBS stabilisation energies are large, much larger than previous estimates. Let us recall here that the MP2/6-31G** calculations yielded for the benzene···hexafluorobenzene complex stabilisation energy of about 4 kcal mol^{-1},[4] and the present CBS values are about twice larger. Furthermore, when passing from the fluoro- to the cyano-isomer, the MP2 stabilisation energy significantly increases, namely from 8.5 to 15.7 kcal mol^{-1}, *i.e.* by almost 90%.

We have shown previously[23] that stacking of nucleic acid bases is systematically connected with a repulsive value of the CCSD(T) correction term and the largest value was found for the stacked methyl adenine···methyl thymine pair (3.6 kcal mol^{-1}). Table 2 shows that the same is true for all the presently considered complexes and the value of correction term increases from the hexafluorobenzene to the hexabromobenzene (the CCSD(T) correction term for the hexacyanobenzene is slightly smaller). The CCSD(T) correction term for the hexabromobenzene complex is by far the largest among all the existing values. It is thus clear that the repulsion character of the CCSD(T) correction term is not connected with the nature of the pair (DNA base pairs) but with the geometrical motif of the pair (stacked motif). The final total stabilisation energies are thus smaller than the MP2/CBS ones but they are still substantial. The largest value (more than 11 kcal mol^{-1}) was determined for the hexacyanobenzene complex, followed by the hexachlorobenzene and hexabromobenzene complexes. A large repulsive CCSD(T) correction term for the hexabromobenzene complex explains the fact that the total stabilization energy of this complex is smaller than that of the hexachlorobenzene complex.

Passing from the fluorobenzene to the bromobenzene, it was found that the MP2 stabilisation energy of stacked dimers increases significantly, and the natural question arises what happens when the iodobenzene is considered. In this case, the relativistic effects play a role, and the non-relativistic calculations used for the above-mentioned complexes cannot be applied. Table 2 summarises the MP2/SDD** results (effectively covering the relativistic effects for bromobenzene and iodobenzene) for all complexes. A direct comparison between the CBS and MP2/SDD** values is difficult since very different basis sets were used and for Br and I effective pseudopotentials are adopted. Despite this similarity of the SDD** and CCSD(T)/CBS interaction energies should be mentioned. It is particularly important that in both calculations the bromobenzene···benzene stabilization energies are smaller than that of chlorobenzene···benzene. This trend follows even for the hexaiodobenzene complex (SDD** calculations) where the relativistic effects play a role. Investigating the MP2/SDD** stabilisation energies, we found that they increase from F to Cl but decrease for I. We can thus conclude that the relativistic effects are responsible for the lower stabilization of the hexaiodobenzene complex. It means that the highest all-electron stabilisation energies for $C_6H_6\cdots C_6X_6$ (X = F, Cl, Br, CN) stacked complexes detected for the benzene···hexabromobenzene and benzene···hexacyanobenzene complexes are reliable, and due to relativistic effects the stabilization energy of the benzene···hexaiodobenzene complex will be smaller.

Table 3 shows the SAPT decomposition of the total interaction energies for selected heterodimers. The electrostatic E^1_{pol} term is systematically stabilizing for all clusters studied but its value for the benzene dimer is negligible. The larger value of the term for the hexafluorobenzene complex (in comparison with the hexachlorobenzene complex) is due to the smaller value of the quadrupole moment of the latter subsystem. The quadrupole moment of the hexacyanobenzene is the largest among all benzene derivatives, and in agreement with that the E^1_{pol} term is the largest for the hexacyanobenzene complex. The first order interaction energy (the sum of polarization and exchange-repulsion terms, E^1 in Table 3) is, however, systematically repulsive what is due to a rather large repulsion value of the exchange-repulsion term. Second-order induction term is surprisingly large but summing this term with its exchange counterpart we obtain negligible contribution. The only exception is the hexacyanobenzene complex where the sum

Table 3 The SAPT decomposition of interaction energy of the stacked structures of the $C_6H_6\cdots C_6X_6$ (X = H, F, Cl, Br, CN) complexes (energies in kcal mol^{-1})

	E^1_{pol}	E^1_{exch}	E^1	E^2_{ind}	$E^2_{ind\text{-}exch}$	E^2_{disp}	$E^2_{disp\text{-}exch}$	E^2	ΔHF	E_{INT}
H	−0.74	5.96	**5.32**	−2.09	1.94	−7.12	1.06	**−6.21**	−0.16	**−1.14**
F	−6.36	12.12	**5.76**	−6.83	6.47	−11.32	1.72	**−9.95**	−0.51	**−4.70**
Cl	−5.41	10.59	**5.19**	−4.70	4.26	−13.99	1.77	**−12.67**	−0.50	**−7.98**
CN	−8.97	11.1	**2.14**	−5.95	4.30	−13.45	1.63	**−13.47**	−0.55	**−11.88**

of these two terms is attractive by 1.6 kcal mol^{-1}. Following expectation, the second-order dispersion term is large and passing from the benzene to the fluoro-, chloro- and the cyano derivatives yields its significant increase. The dispersion energy for the hexachlorobenzene and the hexacyanobenzene complexes is similar, what is slightly surprising in the light of the much larger polarizability of the cyanobenzene. The exchange-dispersion term is systematically small. The second-order interaction energies (E^2 in Table 3) are for all complexes attractive and their major part originates in dispersion energy. Putting all energy terms (including the ΔHF one) together we obtain the total interaction energy which should be compared with the sum of ΔE^{MP2} (aug-cc-pVDZ) and $\Delta E^{CCSD(T)}$ energies. The SAPT stabilisation energy is slightly smaller (by 0.4 kcal mol^{-1}) for the $C_6H_6\cdots C_6F_6$ complex and larger (by 1.2 and 2.6 kcal mol^{-1}) for $C_6H_6\cdots C_6Cl_6$ and $C_6H_6\cdots C_6(CN)_6$ complexes, respectively. The differences are not dramatical and agreement between both stabilization energies is satisfactory.

Conclusion

There main conclusions from this work are:

(i) The CCSD(T)/CBS stabilisation energies of $C_6H_6\cdots C_6X_6$ (X = F, Cl, Br, I, CN) complexes are very large (between 6.3 and 11.0 kcal mol^{-1}), much larger than previously determined.

(ii) The largest stabilisation energy found for the benzene···hexacyanobenzene complex is a result of attractive dispersion and electrostatic quadrupole–quadrupole energies. For all the complexes investigated, the dispersion energy represents the dominant attractive contribution. A large attraction in the stacked arrangement requires a concerted (attractive) action of electrostatic and London dispersion contributions. A rather large attraction originating from polarization and induction contributions is compensated by their exchange counterparts.

(iii) The stabilisation energy of the benzene···hexaiodobenzene is lower than that of the Br isomer, which is explained by relativistic effects.

The stabilisation energies of the stacked complexes are substantial, which suggests that this motif and these constructing blocks may be considered as a powerful tool in supramolecular construction requiring the stable orientation of molecular subsystems. The $C_6H_6\cdots C_6X_6$ (X = F, Cl, Br, I, CN) recognition motif shows a significant stabilization well comparable with hydrogen bonding. The stacking interactions thus exhibit comparable supramolecular activity as hydrogen bonding which was believed to be the only recognition factor.

Acknowledgements

This study was supported by Grants No. LC512 and 203/05/0009 from the Ministry of Education (MSMT) of the Czech Republic and the Grant Agency of the Czech Republic and it was a part of the research project No. Z4055905. It was supported also by grant No. MSM6198959216 (PJ) from the MSMT of the Czech Republic.

References

1 K. Müller-Dethlefs and P. Hobza, *Chem. Rev.*, 2000, **100**, 143.
2 M. O. Sinnokrot and C. D. Sherill, *J. Am. Chem. Soc.*, 2004, **126**, 7690.
3 J. H. Williams, *Acc. Chem. Res.*, 1993, **26**, 593.
4 A. P. West, Jr, S. Mecozzi and D. A. Dougherty, *J. Phys. Org. Chem.*, 1997, **10**, 347.
5 S. Bacchi, M. Benaglia, F. Cozzi, F. Demartin, G. Filippini and A. Gavezzotti, *Chem.–Eur. J.*, 2006, **12**, 3538.
6 (*a*) J. Šponer and P. Hobza, *Collect. Czech. Chem. Commun.*, 2003, **68**, 2231; (*b*) P. Hobza and J. Šponer, *Chem. Rev.*, 1999, **99**, 3247.
7 A. Halkier, T. Helgaker, P. Jorgensen, W. Klopper, H. Koch and J. Olsen, *Chem. Phys. Lett.*, 1998, **286**, 243–252.
8 A. Halkier, T. Helgaker, P. Jorgensen, W. Klopper and J. Olsen, *Chem. Phys. Lett.*, 1999, **302**, 437.
9 T. H. Dunning, *J. Chem. Phys.*, 1989, **90**, 1007.
10 P. Jurečka and P. Hobza, *J. Am. Chem. Soc.*, 2003, **125**, 15608.
11 P. Jurečka and P. Hobza, *Chem. Phys. Lett.*, 2002, **365**, 89.
12 I. Dąbkowska, P. Jurečka and P. Hobza, *J. Chem. Phys.*, 2005, **122**, 204322.
13 A. Hesselmann, G. Jansen and M. Schütz, *J. Chem. Phys.*, 2005, **122**, 014103.
14 B. Jeziorski, R. Moszynski and K. Szalewicz, *Chem. Rev.*, 1994, **94**, 1887.
15 A. Hesselmann and G. Jansen, *Chem. Phys. Lett.*, 2002, **362**, 319.
16 A. Hesselmann and G. Jansen, *Chem. Phys. Lett.*, 2003, **367**, 778.
17 A. Hesselmann and F. R. Manby, *J. Chem. Phys.*, 2005, **123**, 164116.
18 R. Podeszva, R. Bukowski and K. Szalewicz, *J. Chem. Theory Comput.*, 2006, **2**, 400.
19 M. Grünig, O. V. Gritsenko, S. J. A. van Ginsbergen and E. J. Baerends, *J. Chem. Phys.*, 2001, **114**, 652.
20 M. J. Frisch, G. W. Trucks, H. B. Schlegel, G. E. Scuseria, M. A. Robb, J. R. Cheeseman, J. A. Montgomery Jr, T. Vreven, K. N. Kudin, J. C. Burant, J. M. Millam, S. S. Iyengar, J. Tomasi, V. Barone, B. Mennucci, M. Cossi, G. Scalmani, N. Rega, G. A. Petersson, H. Nakatsuji, M. Hada, M. Ehara, K. Toyota, R. Fukuda, J. Hasegawa, M. Ishida, T. Nakajima, Y. Honda, O. Kitao, H. Nakai, M. Klene, X. Li, J. E. Knox, H. P. Hratchian, J. B. Cross, V. Bakken, C. Adamo, J. Jaramillo, R. Gomperts, R. E. Stratmann, O. Yazyev, A. J. Austin, R. Cammi, C. Pomelli, J. W. Ochterski, P. Y. Ayala, K. Morokuma, G. A. Voth, P. Salvador, J. J. Dannenberg, V. G. Zakrzewski, S. Dapprich, A. D. Daniels, M. C. Strain, O. Farkas, D. K. Malick, A. D. Rabuck, K. Raghavachari, J. B. Foresman, J. V. Ortiz, Q. Cui, A. G. Baboul, S. Clifford, J. Cioslowski, B. B. Stefanov, G. Liu, A. Liashenko, P. Piskorz, I. Komaromi, R. L. Martin, D. J. Fox, T. Keith, M. A. Al-Laham, C. Y. Peng, A. Nanayakkara, M. Challacombe, P. M. W. Gill, B. Johnson, W. Chen, M. W. Wong, C. Gonzalez and J. A. Pople, *GAUSSIAN 03 (Revision A.1)*, Gaussian Inc, Wallingford CT, 2003.
21 R. Ahlrichs, M. Bär, M. Häser, H. Horn and C. Kölmel, *Chem. Phys. Lett.*, 1989, **162**, 165.
22 *MOLPRO*, a package of *ab initio* programs designed by H.-J. Werner and P. J. Knowles, version 2002.1, R. D. Amos, A. Bernhardsson, A. Berning, P. Celani, D. L. Cooper, M. J. O. Deegan, A. J. Dobbyn, F. Eckert, C. Hampel, G. Hetzer, P. J. Knowles, T. Korona, R. Lindh, A. W. Lloyd, S. J. McNicholas, F. R. Manby, W. Meyer, M. E. Mura, A. Nicklass, P. Palmieri, R. Pitzer, G. Rauhut, M. Schütz, U. Schumann, H. Stoll, A. J. Stone, R. Tarroni, T. Thorsteinsson and H.-J. Werner.
23 P. Jurečka, J. Šponer, J. Černá and P. Hobza, *Phys. Chem. Chem. Phys.*, 2006, **8**, 1985.

Appendix B

K. Pluháčková and P. Hobza, "On the nature of surprisingly small (red) shift in the halothane....acetone complex", *ChemPhysChem, in press (2007)*

On the nature of the surprisingly small (red) shift in the halothane...acetone complex

Kristýna Pluháčková and Pavel Hobza*

Institute of Organic Chemistry and Biochemistry, Academy of Sciences of the Czech Republic and Centre for Biomolecules and Complex Molecular Systems, Flemingovo nám. 2, 166 10 Prague 6, Czech Republic; e-mail: pavel.hobza@uochb.cas.cz

Dedicated to the memory of Camille Sandorfy, my first post-doctoral adviser and my esteemed friend, who was among the first who recognized the blue-shifting H-bonding experimentally

Halothane...acetone and fluoroform...acetone complexes were studied using the MP2 method with a cc-pVTZ basis set and the DFT method with a TZVP basis set. Whereas upon complexation halothane exhibits a small red shift, fluoroform shows a pronounced blue shift. To explain this difference in behaviour, we performed the SAPT and NBO analyses. Although the composition of the total stabilisation energy of each complex was different, that alone did not provide a satisfactory explanation for the difference in the spectral shifts. The origin of the difference in the shifts was interpreted to be a result of the interplay of the hyperconjugation and rehybridisation mechanisms. The small and surprisingly red shift of the C-H stretch frequency of halothane resulting from the complexation of halothane with acetone was explained by the compensation of the two above-mentioned mechanisms. On the other hand, the fluoroform...acetone complex exhibited a blue shift of the C-H stretch frequency upon complexation, the reason for which in this case was most likely that hyperconjugation as well as rehybridisation mechanisms acted in concert. The calculated shift of the C-H stretch vibration frequencies of halothane (+27 cm^{-1}) agreed with the experimental value of +5 cm^{-1}.

Keywords: blue-shifting H-bonding, nature of bonding, halothane...acetone, fluoroform...acetone

1. Introduction

A hydrogen(H)-bond is a non-covalent bond between the electron-deficient hydrogen and a region of high electron density. Most frequently, an H-bond is of the X-H...Y type, where X is the electronegative element and Y is a place with an excess of electrons. The formation of an H-bond is accompanied by changes in the properties of the X-H covalent bond. Until very recently, it was believed that this bond systematically weakens (upon complex formation), which is manifested by an elongation of the bond and a shift to lower X-H stretch vibration frequencies. A shift to lower frequencies, a so-called red shift, is the most important, easily detectable manifestation of H-bond formation. Red shift used to be dogma, witnessed by the fact that none of the three books on H-bonding published at the end of the last century[1-3] admitted the existence of any shift other than the red one. The first systematic investigation of the other one, i.e. the blue shift of the X-

H stretch frequency upon complex formation, was carried out as a part of our theoretical study of the interaction of benzene with C-H proton donors.[4] We are now aware that the first experimental evidence on the blue shift appeared even before our paper, namely that several papers, independently of one another, mentioned the existence of the blue shift upon complex formation.[5-9] One of the earliest proofs was obtained in 1980 in the Sandorfy laboratory in Montreal. The authors[5] measured how fluoroparafins containing the $-CHF_2$ groups associate with various proton acceptors and found a shift of the frequency in the C-H stretch to higher values. Fluoroparafins, or more generally the halogenated hydrocarbons, act as general anaesthetics, and their action is explained by perturbing non-covalent interactions, mainly H-bonding. Halothane (2-bromo-2-chloro-1,1,1-trifluoroethane) is among the most potent and most widely-used general anaesthetics.

The nature of blue-shifting H-bonding, unlike that of H-bonding in general, is still not fully understood. At least four explanations exist ranging from hyperconjugation, electrostatic model (the role of electric field), repulsion-wall hypothesis through to rehybridisation.[10-15] The single model explains the blue-shifting phenomenon in a particular complex or a class of complexes, whereas the universal model (still non-existent) would collect features of all the various models possible. The combination of hyperconjugation and rehybridisation models suggested by Alabugin et al.[13,14] seems to be the most successful in providing an explanation of blue-shifting H-bonding in the case of polar subsystems.

The vibration spectra of halothane and its complexes with acetone and dioxane have recently been measured.[16] Contrary to expectation, the C-H stretch frequencies of halothane complexes shifted to the red (when compared with the isolated halothane in CCl_4), but the red shifts were rather small (between 6 and 16 cm^{-1}). This finding was unexpected, because mostly blue shifts had been detected for halogenated hydrocarbons. Experimental C-H spectral shifts for several complexes with halogenated hydrocarbons possessing the C-H...O or C-H...π binding motifs are, for the sake of comparison, shown in Table 1.

In order to explain the surprising existence of the red shift in halothane complexes, we decided to investigate its origin in details. Among other reasons for such a study, it might also shed more light on the origin of the blue-shifted H-bonds, which, despite enormous theoretical and experimental effort, has still not been fully understood. In this study, we will investigate bonding in the halothane...acetone complex and, for the sake of comparison, also in the fluoroform...acetone complex. It should be emphasised that fluoroform complexes exhibit a pronounced blue-shifted H-bond.

2. Methods

Both subsystem (halothane, fluoroform, acetone) and complex (halothane...acetone, fluoroform...acetone) geometries were optimised at the RI-MP2/cc-pVTZ and DFT/TPSS/TZVP levels, adopting the standard gradient optimisation technique. The stabilisation energies of the two complexes were determined at each of the levels, including the basis set superposition error (BSSE) a posteriori. Harmonic vibration frequencies were obtained at the same theoretical level, with no scaling adopted.

In the DFT-SAPT method,[17] the interaction energy is given as the sum of first- and second-order energies ($E^{(1)}$, $E^{(2)}$) as well as the δ(HF) term. The first energy contains electrostatic ($E_{el}^{(1)}$) and exchange-repulsion ($E_{ex}^{(1)}$) contributions, whereas the latter consists of the induction, exchange-induction, dispersion and exchange-dispersion contributions. Accordingly, second-order exchange components will be added into the

induction ($E_{in}^{(2)}$) and dispersion ($E_d^{(2)}$) terms. The δ(HF) term estimates higher-order Hartree-Fock (HF) contributions (induction, exchange-induction and charge-transfer). We used PBE0AC exchange-correlation functional with density fitting and the aug-cc-pVDZ basis set for the decomposition. The aug-cc-pVDZ set is large enough to provide a reliable estimate of the electrostatic, induction and exchange components. The dispersion component is underestimated by about 10–20% in this basis set but should serve well enough for the purpose of comparison. We implemented a gradient-controlled shift procedure, which needs a difference (shift) between the vertical ionisation potential (IP) and HOMO energy of the DFT method used as an input.[17] The IPs were calculated at the PBE0/TZVP level while the HOMO values were taken from the aug-cc-pVDZ calculation.

To learn more about the nature of complexation, the Natural Bond Orbital (NBO) analysis was performed. The method is fully defined only when based on HF and DFT characteristics. The NBO characteristics of both complexes were determined at the DFT/B3-LYP/cc-pVTZ level.

All calculations were performed with TURBOMOLE[18] and GAUSSIAN03.[19]

3. Results and Discussion

Isolated subsystems. Figure 1 and Table 2 show the structure, geometry, dipole moments and selected stretch vibration frequencies of isolated subsystems. The dipole moment of fluoroform, which is larger than that of halothane, indicates that electrostatic interactions in the halothane...acetone complex will be weaker than in the fluoroform...acetone complex.

A very important property which frequently determines the character of the H-bonding is the derivative of the molecule dipole moment with respect to the change in the X-H bond length. This derivative is mostly positive, which means that an increase in the dipole moment is connected with an elongation of the X-H bond. Several systems exhibit, however, the opposite feature, namely the dipole-moment increase is connected with a contraction of the X-H bond. We had already discovered this in 1998 when investigating the fluoroform...ethylene oxide complex[20], where contraction of the C-H bond of the fluoroform upon complexation was responsible for the blue shift of the C-H stretch frequency. The dipole moment of (optimised) fluoroform amounts to 1.67 D; the elongation and contraction of the C-H bond (by 0.1 Å) yield a dipole moment of 1.61 and 1.71 D, respectively. The situation of halothane, however, is rather peculiar. The dipole moment of (optimised) halothane is 1.24 D. In this case, both elongation and contraction of the C-H bond (again by 0.1 Å) result in a dipole-moment increase (to 1.39 and 1.35 D), i.e. slightly larger for elongation. It should be mentioned that we are not aware of any other molecule exhibiting this feature, and the interpretation in the case of halothane is not straightforward. It should be repeated that it is the contraction of the X-H bond in proton donor that is responsible for the blue shift of the C-H stretch frequency upon complex formation, whereas it is elongation of the bond that explains the red shift.

Complexes. Figure 2 and Table 3 show the structure, geometry and selected stretch vibration frequencies of the fluoroform...acetone and halothane...acetone complexes determined at the MP2 level. The C-H...O H-bond in the halothane...acetone complex is nearly linear, and the distance between the heavy atoms (3.09 Å) indicates an existence of rather strong bonding. This is confirmed by substantial stabilisation energy of the complex, amounting to 5 kcal/mol. It should be mentioned that stabilisation energy of the water dimer possessing a strong O-H...O H-bond is practically identical. The C-H bond in halothane is slightly contracted upon complexation (by 0.0023 Å), and this bond

contraction usually indicates a blue shift of the C-H stretch frequency. Surprisingly enough, the resulting C-H stretch vibration frequency is red-shifted, and this shift is not negligible (27 cm^{-1}). Halothane thus behaves like most other CH donors with respect to its bond length changes but is anomalous in terms of stretching frequency changes. The C=O bond in acetone is also contracted upon complexation (by 0.005 Å), but its stretch frequency is red-shifted only slightly (by 3 cm^{-1}). DFT calculations (cf Table 3) predict elongation of the C-H bond of halothane together with the red shift of its stretch vibration. Due to the fact that DFT calculations do not cover the London dispersion energy the molecular characteristics (geometry and stabilization energy) might be incorrect. From this point of view we cannot rely on the DFT results.

When we compare the characteristics of this complex with those of fluoroform...acetone, it is evident from Figure 2 that also this complex exhibits a practically linear C-H...O H-bond, and also the distance of the heavy atoms is comparable (3.26 Å). The C-H bond is contracted upon complexation, and the contraction is similar as in the case of the previous complex. Performing the vibration analysis we found, however, a pronounced blue shift of 36 cm^{-1}. The stabilisation energy of the fluoroform...acetone complex is slightly smaller (3.66 kcal/mol) than that of the halothane...acetone complex, but the difference is not substantial and cannot explain the different spectral behaviour of the two complexes. However, when investigating the composition of the stabilisation energies, we found a significant difference. The correlation part of the stabilisation energy of the halothane complex amounted to 3.3 kcal/mol while in the case of the fluoroform complex it was only 0.2 kcal/mol. Furthermore, the HF stabilisation energy of the halothane complex (1.66 kcal/mol) was considerably smaller than that of the fluoroform complex (3.45 kcal/mol). These numbers indicate that the binding in the halothane complex originated in the correlation energy, whereas in the case of the fluoroform complex it came from the HF energy.

Different stability of both complexes is discussed in terms of C-H....O H-bonds and question remains which role is played by other C-H...F and C-H...Cl H-bonds. Intermolecular H...F and H...Cl distances in fluoroform...acetone and halothane...acetone complexes are 2.60 and 3.15 Å, respectively. These distances are too large for formation of an H-bond. Further, the NBO analysis (see later) clearly tells us that there is no hyperconjugation to C-F and C-Cl antibonding orbitals of fluoroform and halothane, respectively what indicate that the respective H-bond is not formed.

Finally, we would like to mention that the C-H mode in the C-H...O H-bonds is in both complexes fairly localized. The purity of the C-H stretch is practically not changed when passing from monomer (fluoroform, halothane) to the respective complex.

SAPT analysis. To understand the difference in the nature of the stabilisation of the halothane...acetone and fluoroform...acetone complexes, we performed the DFT-SAPT calculations, and the respective energies are shown in Table 4. Total interaction energies differed slightly from the variation values given in Table 3. It should be, however, noted that the main goal of the SAPT calculations was to provide energy components and not accurate total interaction energies. The difference mentioned can be explained by different basis sets used in the variation (cc-pVTZ) and perturbation (aug-cc-pVDZ) calculations. Investigating the entries in Table 4, we found comparable (attractive) electrostatic energies but significantly different exchange-repulsion energies for both complexes. Consequently, the $E^{(1)}$ energies were attractive for the fluoroform...acetone complex but repulsive for the halothane...acetone complex. The difference was significant, more than 4 kcal/mol in favour of the fluoroform complex. For both complexes, the second-order induction energies were rather small, and significant stabilisation originated in the second-order dispersion energies. The dispersion energy for

the halothane complex was more than twice as large as that for the fluoroform complex, and the drop in its stability, for which the first-order energy was responsible, was fully compensated by the gain from the second-order energy. Considerably larger dispersion energy for the halothane complex is not surprising since polarizability of halothane is about four-times larger than that of fluoroform (44 and 12 a.u.; MP2/cc-pVDZ calculations). The DFT-SAPT energy components fully supported the decomposition of the variation interaction energy mentioned in the previous paragraph. On the basis of energy decomposition we were, however, not able to deduce the nature of the spectral shift of the proton donor upon complexation. Evidently, the subtle differences in the C-H stretch frequencies cannot be explained on the basis of total interaction energies or their components.

NBO analysis. Table 3 shows that MP2 and DFT characteristics of both complexes are similar, which is also true for the spectral shifts. The DFT blue shift in the fluoroform...acetone complex is slightly smaller than the MP2 one, whereas the DFT red shift in the halothane...acetone complex is larger than the MP2 one. This finding is important as it indicates that it is possible to use the DFT technique in the subsequent NBO analysis.

First, the charge transfer (CT) deduced from the NBO atomic charges will be discussed. Both complexes exhibit the same trend of CT, a flow from acetone to proton donor. The CT of halothane is 0.013 e while the CT in the case of fluoroform is about one half (0.007 e). Different magnitudes of the CT are reflected by different stabilisation energies of both complexes, and although these characteristics are not exactly proportional, this ratio implies an important role of charge-transfer-based energy contributions. Investigating the second-order charge-transfer energies in both complexes, we found a dominant contribution from the acetone oxygen lone pair $\rightarrow$ C-H σ^* antibonding orbital of the proton donor. This term is approximately two times larger for the halothane complex (5.1 and 2.6 kcal/mol). When analysing the nominators and denominators in the respective energy term, we realised that the energy difference (denominator) is in both complexes very similar, whereas the matrix element in the nominator which reflects the geometry of both subsystems is larger for the halothane complex. Evidently, the more favourable geometrical arrangement of the halothane...acetone complex (not its better donor-acceptor properties) is responsible for the higher stabilisation energy of the halothane complex.

In the following step, we will study the changes of the energy difference (ED) in orbitals participating in H-bonding. The ED in the C-H σ^* antibonding orbital of the fluoroform decreases (by 0.0011 e) upon complexation with acetone, which indicates the strengthening and contraction of the bond. These effects are connected with the blue shift of the C-H stretch frequency. Investigating the ED in other σ^* antibonding orbitals in fluoroform, we found even larger decrease (by 0.0026 e) in two of three C-F orbitals. The decrease of the ED in C-H and two C-F σ^* antibonding orbitals is compensated by an ED increase in lone electron pairs of all three fluorines. The overall picture is thus the same as we know it from other fluoroform...proton acceptor complexes. Fluoroform is an electron acceptor, but the ED increase is localised at fluorine lone electron pairs. This ED increase is accompanied by a decrease of the ED in the C-H σ^* antibonding orbital, leading to bond contraction and a blue shift of the respective stretch frequency.

The situation is different in the halothane complex, where we found the opposite effect. The ED in the C-H σ^* antibonding orbital of halothane dramatically increased (by 0.0060 e), which implies a weakening and elongation of the bond, connected with the red shift of the C-H stretch vibration frequency. Both calculations and experiment suggest the red shift, but the problem is with the absolute values of this shift. The change of the ED

in the C-H σ* antibonding orbital of halothane is about six times larger than that in fluoroform. Consequently, larger spectral shifts can be expected in the halothane complex. From Table 1 we learned, however, that this is not true and the absolute shift is larger in the fluoroform complex. These numbers clearly show that the mechanism of the H-bonding in both complexes will be different and another mechanism should play a role in addition to the hyperconjugation mechanism.

To explain this difference, we investigated the changes in hybridisation upon complex formation as suggested by Alabugin et al.[13,14] The carbon in isolated halothane possesses $sp^{2.60}$ hybridisation. Upon complexation, the hybridisation decreases to $sp^{2.35}$. The lowering of the hybridisation is connected with the strengthening of the bond and its contraction. Having performed the same analysis for the fluoroform, we found a similar, albeit slightly smaller trend: the carbon hybridisation decreases upon complexation from $sp^{2.30}$ to $sp^{2.15}$. When the two effects (hyperconjugation and rehybridisation) were put together, we found their action to be in concert in the case of the fluoroform complex while in the case of the halothane complex the effects acted in opposing directions. Evidently, the halothane...acetone complex is characterised by the compensation of a substantial hyperconjugation mechanism leading to a red shift of the C-H stretch frequency on the one hand and of a substantial rehybridisation mechanism leading to a blue shift of the C-H stretch frequency on the other. The resulting calculated shift is small and red, which agrees with the experimental finding. In the case of the fluoroform complex, both mechanisms work together, with the resulting shift being blue and relatively large.

4. Conclusions

- Halothane is, to our knowledge, the first system exhibiting both positive and negative dipole-moment derivatives. This means that the dipole moment of halothane increases whether the C-H bond length increases or decreases. On the basis of this behaviour, one cannot expect a pronounced spectral shift (either red or blue) of halothane upon complexation. The same will hold true for any system behaving in the same way.

- The calculated spectral shift of the halothane...acetone complex agrees well with the experimental data.

- The surprisingly small red shift of the C-H stretch frequency of halothane resulting from complexation with acetone was explained by the compensation of hyperconjugation and rehybridisation mechanisms.

- The fluoroform...acetone complex exhibited a blue shift of the C-H stretch frequency upon complexation, and in this case both hyperconjugation and rehybridisation mechanisms acted in concert.

- The origin of blue-shifting H-bonding in various types of complexes formed by polar as well as nonpolar subsystems is explained by the hyperconjugation/rehybridisation model of Alabugin et al.[13,14] and the repulsion-wall model introduced in Ref. 4.

Acknowledgements

This study was supported by Grants No. LC512 and A400550510 from the Ministry of Education (MSMT) of the Czech Republic and the Grant Agency of the Academy of Sciences of the Czech Republic and it was a part of the research project No. Z4055905.

References

1. G. A. Jeffrey, *An introduction to hydrogen bonding*. Oxford University Press, New York, **1997**.
2. G. R. Desiraju, T. Steiner, *The weak hydrogen bond*. Oxford University Press, Oxford, **1999**.
3. S. Scheiner, *Hydrogen bonding*. Oxford University Press, New York, **1997**.
4. P. Hobza, V. Špirko, H. L. Selzle, E. W. Schlag, *J. Phys. Chem. A* **1998**, 102, 2501.
5. G. T. Trudeau, J.-M. Dumas, P. Dupuis, M. Guerin, C. Snadorfy, *Top. Curr. Chem.* **1980**, 93, 91.
6. N. P. Resaev, K. Szczepaniak, *Opt. Spectr. (USSR)* **1964**, 16, 43.
7. S. Pinchas, *J. Phys. Chem.* **1963**, 67, 1862.
8. M. Buděšinský, P. Fiedler, Z. Arnold, *Synthesis* **1989**, 858.
9. I. E. Boldeskul, I. F. Tsymbal, E. V. Rylstev, Z. Latajka, A. J. Barnes, *J. Mol. Struc.* **1997**, 436, 167.
10. P. Hobza, Z. Havlas, *Chem. Rev.* **2000**, 100, 4253.
11. A. Masunov, J. J. Dannenberg, R. H. Contreras, *J. Phys. Chem. A* **2001**, 105, 4737.
12. L. Pejov, K. Hermansson, *J. Chem. Phys.* **2003**, 119, 313.
13. I. V. Alabugin, M. Manoharan, S. Peabody, F. Weinhold, *J. Am. Chem. Soc.* **2003**, 125, 5973.
14. I. V. Alabugin, M. Manoharan, F. Weinhold, *J. Phys. Chem. A* **2004**, 108, 4270.
15. A. Karpfen, E. S. Kryachko, *Chem. Phys. Lett.* **2006**, 431, 428.
16. B. Czarnik-Matusewicz, D. Michalska, C. Sandorfy, Th. Zeegers-Huyskens, *Chem. Phys.* **2006**, 322, 331.
17. A. Hesselmann, G. Jansen, *Phys. Chem. Chem. Phys.* **2003**, 5, 5010, and references therein.
18. R. Ahlrichs, M. Bär, M. Häser, H. Horn, C. Kölmel, *Chem. Phys. Lett.* **1989**, 162, 165.
19. Gaussian 03, Revision A.1, M. J. Frisch, G. W. Trucks, H. B. Schlegel, G. E. Scuseria, M. A. Robb, J. R. Cheeseman, J. A. Montgomery, Jr., T. Vreven, K. N. Kudin, J. C. Burant, J. M. Millam, S. S. Iyengar, J. Tomasi, V. Barone, B. Mennucci, M. Cossi, G. Scalmani, N. Rega, G. A. Petersson, H. Nakatsuji, M. Hada, M. Ehara, K. Toyota, R. Fukuda, J. Hasegawa, M. Ishida, T. Nakajima, Y. Honda, O. Kitao, H. Nakai, M. Klene, X. Li, J. E. Knox, H. P. Hratchian, J. B. Cross, V. Bakken, C. Adamo, J. Jaramillo, R. Gomperts, R. E. Stratmann, O. Yazyev, A. J. Austin, R. Cammi, C. Pomelli, J. W. Ochterski, P. Y. Ayala, K. Morokuma, G. A. Voth, P. Salvador, J. J. Dannenberg, V. G. Zakrzewski, S. Dapprich, A. D. Daniels, M. C. Strain, O. Farkas, D. K. Malick, A. D. Rabuck, K. Raghavachari, J. B. Foresman, J. V. Ortiz, Q. Cui, A. G. Baboul, S. Clifford, J. Cioslowski, B. B. Stefanov, G. Liu, A. Liashenko, P. Piskorz, I. Komaromi, R. L. Martin, D. J. Fox, T. Keith, M. A. Al-Laham, C. Y. Peng, A. Nanayakkara, M. Challacombe, P. M. W. Gill, B. Johnson, W. Chen, M. W. Wong, C. Gonzalez, and J. A. Pople, Gaussian, Inc., Wallingford CT, **2003**.
20. P. Hobza, Z. Havlas, *Chem. Phys. Lett.* **1999**, 303, 447.

Table 1. Experimental spectral shifts (in cm^{-1}) of various complexes; the positive numbers indicate a blue shift of the C-H stretch vibration upon complexation

	CH_3COCH_3[a]	CH_3COCH_3[b]	C_2D_4O[b]	fluorobenzene[c]
HCF_3	18	27	24	21
$HCClF_2$	14	24	21	-
$HCCl_2F$	5	16	14	-
$HCCl_3$	-8	1	1	14

[a]in liquid argon, Ref. 7; [b]in liquid krypton, Ref. 8; [c]in gas phase, Ref. 9

Table 2. Characteristics of isolated subsystems determined at the RI-MP2/cc-pVTZ level; the numbers in parentheses refer to DFT/TPSS/TZVP calculations

	μ[D]	$\nu_{C\text{-}H}$[cm^{-1}]	$r_{C\text{-}H}$[Å]
Halothane	1.24	3183 (3126)	1.084 (1.087)
Fluoroform	1.67	3204 (3099)	1.085 (1.092)
Acetone	2.97	-	-

Table 3. RI-MP2/cc-pVTZ and DFT/TPSS/TZVP characteristics of the halothane...acetone and fluoroform...acetone complexes; the numbers in parentheses indicate the change upon complexation

		ΔE(kcal/mol)[a]	$r_{C\text{-}H}$[Å]	$\nu_{C\text{-}H}$[cm^{-1}]
Halothane...acetone[b]	MP2	-5.0/-1.7/-3.3	1.082	3156 (-27)
	DFT	-4.2	1.091	3053 (-73)
Fluoroform...acetone[b]	MP2	-3.7/-3.5/-0.2	1.083	3240 (36)
	DFT	-4.0	1.091	3121 (22)

[a]Total interaction energy/HF interaction energy/correlation interaction energy; [b]Cf. Fig. 2

Table 4. The DFT-SAPT analysis for the halothane...acetone and fluoroform...acetone complexes; energies in kcal/mol

	$E^{(1)}_{el}$	$E^{(1)}_{ex}$	$E^{(1)}$	$E^{(2)}_{i}$	$E^{(2)}_{d}$	$E^{(2)}$	δ(HF)	E
Fluoroform...acetone[a]	-6.08	5.36	-0.72	-0.77	-2.42	-3.19	-0.51	-4.41
Halothane...acetone[a]	-5.88	9.77	3.89	-1.55	-5.38	-6.92	-1.31	-4.35

[a]Cf. Fig. 2

Figure 1. Optimised structures of acetone, fluoroform and halothane

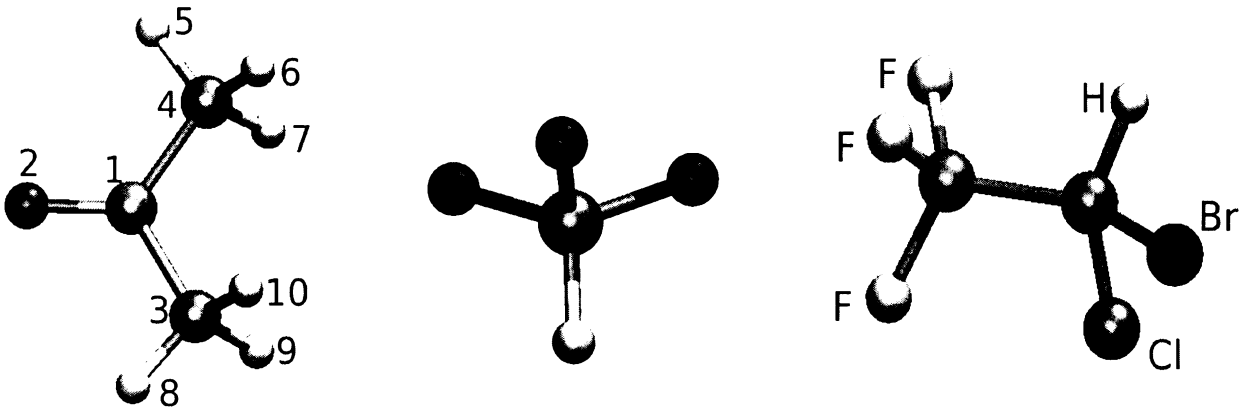

Acetone Fluoroform Halothane

Figure 2. Optimised structures of the halothane...acetone and fluoroform...acetone complexes

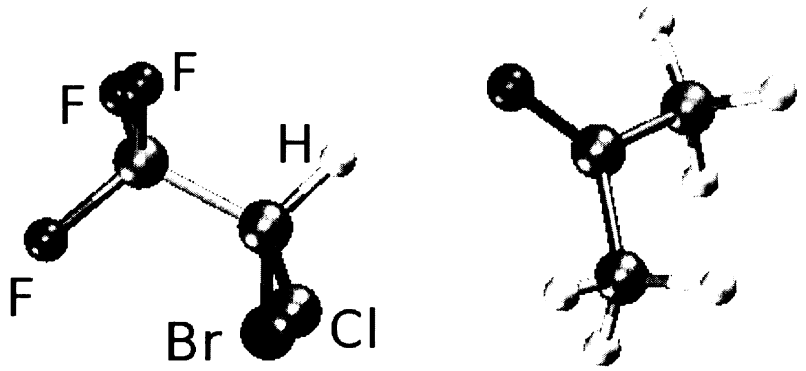

Halothane...acetone

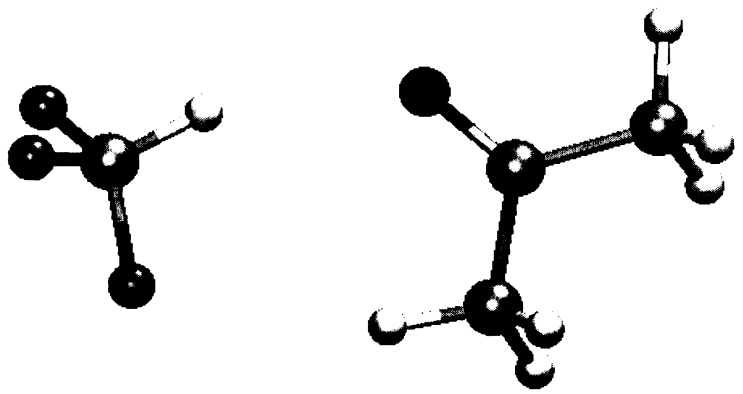

Fluoroform...acetone